



Università
degli Studi
di Catania



Università degli Studi di Catania
Scuola Superiore di Catania

International PhD
in
Translational Biomedicine
XXVI cycle

**Identification and functional analysis of genes
associated with oncogenesis**

Eliana Salvo

Coordinator of PhD

Prof. D. Condorelli

Tutor

Prof. G Rappazzo

a.a. 2010/2013

CONTENTS

ABSTRACT.....	7
INTRODUCTION	9
REPLICATIVE SENESCENCE.....	9
PREMATURE SENESCENCE.....	11
DNA DAMAGE RESPONSE.....	13
OXIDATIVE STRESS AND SENESCENCE.....	15
AUTOPHAGY : BETWEEN LIFE AND DEATH.....	17
THE MITOCHONDRIAL FREE RADICAL THEORY OF AGING.....	19
CANCER AND NEURODEGENERATION, AN INVERSE RELATION.....	20
METALLOTHIONEINS AND OXIDATIVE STRESS.....	22
THE REGION OF MINIMAL DELETION ON CHROMOSOME 6Q26-27.....	27
THE CATP GENE.....	29
IDENTIFICATION OF A NOVEL GENE	30
RESULTS.....	30
<i>CATP</i> EXPRESSION.....	32
MUTATIONAL ANALYSIS.....	33
EVOLUTION.....	37
DISCUSSION	42
EVIDENCES OF <i>CATP</i> AS A NOVEL GENE.....	42
CATP PROTEIN	44
RESULTS.....	44
BIOINFORMATIC PREDICTIONS OF <i>CATP</i> STRUCTURE.....	44
DESIGNING A SYNTHETIC PEPTIDE AND IMMUNIZATION.....	45
IMMUNOHISTOCHEMISTRY	46

IMMUNOFLUORESCENCE	48
DISCUSSION	50
RESULTS.....	51
CLONING	51
DISCUSSION	65
CONCLUSIVE REMARKS	66
<u>MATERIALS AND METHODS.....</u>	<u>68</u>
DNA SAMPLES.	68
PHASING	69
SEQUENCING.....	69
BIOINFORMATIC TOOLS	70
DESIGNING A SYNTHETIC PEPTIDE FOR <i>CATP</i>	70
POLYCLONAL AND MONOCLONAL ANTIBODIES.....	70
CELL CULTURE.	71
IMMUNOCYTOCHEMISTRY.	71
TRANSFORMATION	74
YEAST CULTURE	74
<u>ACKNOWLEDGEMENTS</u>	<u>75</u>
<u>REFERENCES</u>	<u>76</u>

LIST OF FIGURES

Fig. 1 Growth curve of <i>S. cerevisiae</i> culture	25
Fig. 2 Contig of the HD region (from Lin and Morin, 2001).	29
Fig. 3 3YAC contig map encompassing the critical region of the RMD.....	30
Fig. 4 Southern blot analysis of YAC911C10 and Dot blot of derived cosmids.....	31
Fig. 5 RT_PCR on human cell lines.	32
Fig. 6 SNPs mapped to <i>catp</i> sequence.	34
Fig. 7 DHPLC profiles.....	35
Fig. 8 Multiple alignment of <i>catp</i> sequence in primate.	38
Fig. 9 c.34A>T SNP assay fluoresce curves.....	39
Fig. 10 Allelic Discrimination Plot example	40
Fig. 11 Secondary Structure prediction obtained by InterproScan.....	44
Fig. 12 Computation of various physico-chemical properties of CATP obtained by PROSITE.	45
Fig. 13 Immunohistochemistry.	47
Fig. 14 Immunofluorescence in SH-SY5Y cells	49
Fig. 15 chimp allele transformed yeast.....	52
Fig. 16 Colony morphology on Glucose medium: smooth colonies	54
Fig. 17 Colony morphology on Glycerol medium: wrinkly colonies.....	54
Fig. 18 SDGlu-TB plates details.....	55
Fig. 19 SDGly-TB medium	56

Fig. 20 ImageJ elaborated colonies images.	56
Fig. 21 SDGly-TB plate detail of chimp allele	57
Fig. 22 Hydrogen peroxide-mediated inhibition.....	58
Fig. 23 CFU counts after media shift.....	61
Fig. 24 Colonies size on SDGlu.....	62
Fig. 25 ROS production without (up) and after (down) H ₂ O ₂ treatment	63
Fig. 26 pRS415 map	73

LIST OF TABLES

Tab I Collections of mutants in human sample population from Burkina Faso.....	36
Tab II catp alleles: genotypes and allele frequencies.	36
Tab III wild type and c.34A>T variant distribution in different pathological conditions.....	41
Tab IV pRS415 main features.....	73

ABSTRACT

This study begun with the research project “Genetica Molecolare del processo di senescenza” at IRCSS Oasi Maria SS. - Troina (Enna, Italy). That project was aimed to identify genes mapping within the RMD at the 6q26-27 region, which harbored a locus of senescence named *SEN6* (Banga, et al, 1997). It was also known that this region was also implicated with tumorigenesis, since LOH of polymorphic markers were found in some forms of cancer, and a Region of Minimal Deletion (RMD) has been described encompassing markers D6S193-D6S149 (Saito et al., 1992).

One cDNA clone from fetal brain was recovered from a cDNA selection assay and a genomic segment matching the cDNA sequence was identified on chromosome 6 contig. It mapped within the RMD near marker D6S193, and encoded a putative protein without any homology with respect to known sequences. Our aim was to do a functional analysis of this gene in order to evaluate a possible relationships with cancer.

Any functional analysis of gene/protein is normally facilitated by bioinformatic analysis; in this case, however, the lack of homology made the study of its function(s) much more difficult.

Initially, computational studies on the protein were performed which evidenced a possible membrane-binding domain at the C-terminus. For this reason the protein was named CATP (Cytomembrane-Associated Trafficking Protein).

Then, genetic analysis was done to better define *catp* gene. Particularly, mutation were scanned to identify variants and alleles of the gene, and modifications of its sequence across evolution, especially in Great Apes, were evaluated. Alleles were analyzed for association with diseases such as Neurodegenerative disorders, as well as Autistic spectrum disorders, Early Epilepsy and Leukemias.

Finally functional analysis was performed in a simple *in vivo* model, using the yeast *Saccharomyces cerevisiae*, in order to clarify function of *catp* and the different effects of its alleles on yeast chronological lifespan, a measure of aging in postmitotic

tissues. Data suggested that *catp* alleles can affect yeast growth in distinguishable ways. Moreover they showed different sensitivity to oxidative stress compared each other and versus a negative control. So far a possible role of *catp* in senescence and/or tumorigenesis has been suggested through oxidative stress response and ROS level regulation.

Chapter 1

INTRODUCTION

Replicative senescence.

One of the first observations made for primary cells explanted from human tissue was that such cells do not proliferate indefinitely but instead are “mortal”. Hayflick observed that cultured human fibroblasts undergo senescence (a loss of replicative capacity) after a uniform, fixed number of ~50 population doublings, commonly termed the Hayflick limit. Primary cells explanted from human tissue do not proliferate indefinitely but instead are “mortal.” Their proliferative capacity upon explantation consistently displays three phases: phase I, corresponding to a period of little proliferation before the first passage, during which the culture establishes; phase II, characterized by rapid cell proliferation; and phase III, during which proliferation gradually grinds to a complete halt (Hayflick and Moorhead 1961). Commenting on the possible causes of the transition to phase III, Hayflick (1965) hypothesized that “The finite lifetime of diploid cell strains in vitro may be an expression of aging or senescence at the cellular level.” The term cellular senescence therefore denotes a stable and long-term loss of proliferative capacity, despite continued viability and metabolic activity. Almost half a century after the first reports describing the limited replicative potential of primary cells in culture, there is now overwhelming evidence for the existence of “cellular senescence” in vivo.

The absence of telomerase in cultured human cells and the shortening of telomeres at each population doubling have suggested that telomere length acts as a mitotic clock that accounts for their limited lifespan (Rubin, 2002). With the propagation of human cells in culture, telomeres (the protective chromosomal termini) are progressively shortened, ultimately causing cells to reach their “Hayflick limit”.

This barrier has been termed replicative (cellular) senescence, since it is brought about by replication. Telomeres are subject to attrition due to the fact that DNA polymerase fails to completely replicate the lagging strands. In the early 1970s, Olovnikov (1971) and Watson (1972) independently described this so-called “end replication problem”, which contributes to telomere shortening. Thus, telomeres act as a molecular clock, reflecting the replicative history of a primary cell. When telomeres reach a critical minimal length, their protective structure is disrupted. This triggers a DNA damage response (DDR), which is associated with the appearance of foci that stain positive for γ -H2AX (a phosphorylated form of the histone variant H2AX) and the DDR proteins 53BP1, NBS1, and MDC1. Moreover, the DNA damage kinases ATM and ATR are activated in senescent cells. After amplification of the DDR signal, these kinases activate CHK1 and CHK2 kinases. Communication between DDR-associated factors and the cell cycle machinery is brought about by phosphorylation and activation of several cell cycle proteins, including CDC25 (a family of phosphatases) and p53. In addition, differential expression of p53 isoforms has been linked to replicative senescence. Together, these changes can induce a transient proliferation arrest, allowing cells to repair their damage. However, if the DNA damage exceeds a certain threshold, cells are destined to undergo either apoptosis or senescence. The factors bringing about this differential outcome have remained largely elusive, but the cell type and the intensity and duration of the signal, as well as the nature of the damage, are likely to be important determinants (Kuilman, et al., 2010).

The dependence of replicative senescence on telomere shortening is evident from its bypass by the ectopic expression of the catalytic subunit of the telomerase holoenzyme (hTERT), which elongates telomeres, thereby abrogating the effect of the end replication problem (Bodnar et al. 1998). The limited life span of most primary human cells is explained by the fact that, in contrast to stem cells, telomerase is not expressed in human somatic cells, so they are unable to maintain telomeres at a sufficient length to suppress a DDR (Harley et al. 1990; Masutomi et al. 2003). Tumor cells often express telomerase (Shay and Bacchetti 1997), or elongate their telomeres through a mechanism termed alternative lengthening of telomeres (ALT) (Muntoni and Reddel 2005). As a result, telomeres of human cancer cells are maintained at a length

that permits continued proliferation (Shay and Wright 2006).

Senescence is now recognized as a critical feature of mammalian cells to suppress tumorigenesis, acting alongside cell death programs. Cellular senescence acts as a barrier to tumorigenesis. The ability of cells to bypass replicative senescence leads to immortalization, which can promote neoplastic transformation. The phenotype of limited division of the normal human cell has been reported to be dominant over the immortal phenotype of HeLa and SV40-transformed cells in hybrids; cellular immortality was found to be a recessive phenotype in hybrids. Fusion of immortal cell lines with normal human fibroblasts or certain other immortal cell lines yields hybrids having limited division potential. This result also indicated that senescence was the result of active genetic mechanisms rather than random events (Pereira-Smith, 1983).

Premature senescence.

Despite telomere erosion is considered to be the main cause of the onset of replicative senescence, recent findings suggest that a senescent phenotype can be induced by a variety of other stimuli that act independently of telomeres (Itahana, 2004). Premature cellular senescence is the term used to refer to this type of senescence, since it arises prior to the telomere shortening.

Many different mechanisms of premature senescence can occur in cells which can be triggered by exogenous signals such as oncogenic stimuli, DNA damage and oxidative stress. In cultured cells stress-induced senescence, oncogene-induced senescence (OIS) and tumor-suppressor senescence are described. There is now a large number of evidences for premature senescence existence in vivo.

Oncogene-induced senescence

Early studies on mutant HRAS (HRAS^{V12}) led to the discovery that, although it

can transform most immortal mammalian cell lines and collaborate with immortalizing genes in oncogenically transforming primary cells, it induces cell cycle arrest when it is introduced alone into primary cells (and at least one immortal rat fibroblast cell line) (Land et al. 1983; Franza et al. 1986; Serrano et al. 1997). Serrano et al. (1997) noted the striking phenotypic resemblance of such nonproliferating cells to those in replicative senescence, and this phenomenon has eventually come to be known as oncogene-induced senescence (OIS). Unlike replicative senescence, OIS cannot be bypassed by expression of hTERT, confirming its independence from telomere attrition (Wei and Sedivy 1999). Some different studies have provided evidences for OIS in vivo, senescence markers have been demonstrated in several contexts in which oncogenes or tumor suppressor gene were perturbed; e.g. Melanocytic nevi, benign tumors that have a low propensity to progress toward melanoma, are a well-studied system for OIS in vivo in humans, mice, and fish. In 2002, BRAF^{E600} was identified as a frequent mutation in human cancer, predominantly melanoma (Davies et al. 2002). At least as remarkable was the finding that the same mutation is present in the large majority of nevi (Pollock et al. 2003). In spite of the presence of an oncogenic BRAF allele, an important and common feature of nevi is their exceedingly low proliferative activity. This characteristic is typically maintained for decades until the lesion gradually disappears. Nevi express elevated levels of p16^{INK4A} and display increased SA-b-GAL activity (Michaloglou et al. 2005). Arguing against a role for replicative senescence, it was found that telomere length in nevi is indistinguishable from that in normal skin (and longer than in melanoma cells). This strongly suggests that nevi undergo OIS in vivo.

Tumor suppressor loss-induced senescence

Similar to oncogene mutation or overexpression, loss of a tumor suppressor can also trigger senescence in mouse and human cells. Pandolfi and colleagues were the

first to show that senescence *in vivo* can also be triggered by the loss of a tumor suppressor gene. They found that conditional Pten deletion in murine prostate cells results in the formation of high-grade PIN ((prostatic intraepithelial neoplasia), which display characteristics of senescence. In conjunction with p53 loss, these lesions progress to malignancy. Together, these examples provide the first pieces of evidence that, similar to activated oncogenes, loss of expression of tumor suppressors can also cause incipient cancer lesions to activate features of senescence, serving to limit tumorigenesis *in vivo* (Kuilman, 2010).

DNA damage response.

Cellular senescence is associated with ageing and cancer *in vivo* and has a proven tumour-suppressive function. Common to both ageing and cancer is the generation of DNA damage and the engagement of the DNA-damage response pathways (D'Adda di Fagagna 2008).

Structural changes to DNA severely affect its functions, such as replication and transcription, and play a major role in age-related diseases and cancer. A complicated and entangled network of DNA damage response (DDR) mechanisms, including multiple DNA repair pathways, damage tolerance processes, and cell-cycle checkpoints safeguard genomic integrity. Like transcription and replication, DDR is a chromatin-associated process that is generally tightly controlled in time and space. As DNA damage can occur at any time on any genomic location, a specialized spatio-temporal orchestration of this defense apparatus is required. Genomic insults arise from side effects of DNA metabolizing processes, such as replication errors, uncontrolled recombination, off-target mutation induction by somatic hypermutation during antigen production, and inaccurate VDJ recombination (Liu and Schatz, 2009) The biggest genomic burden is, however, induced by processes that directly damage DNA. DNA lesions are derived from three main sources (Lindahl 1993; Friedberg et al. 2006): environmental agents such as ultraviolet light, ionizing radiation, and numerous genotoxic chemicals; reactive oxygen species (ROS) generated by respiration and lipid peroxidation; and spontaneous hydrolysis of nucleotide residues, inducing abasic sites

and deamination of C, A, G, or 5methyl-C. It is estimated that each cell is confronted with approximately 10^4 – 10^5 lesions per day, indicating that clearance of genomic injuries constitutes a demanding task to maintain proper genome function. Essential genome processes, such as transcription and replication, are severely affected by DNA lesions. Replication over damaged DNA induces mutations, which may initiate and propagate carcinogenesis.

To deal with the fundamental problem of genomic erosion, a sophisticated network of DNA damage-response (DDR) systems has evolved. These include a set of DNA repair mechanisms, damage tolerance processes, and cell-cycle checkpoint pathways. The biological significance of a functional DDR for human health is clearly illustrated by the severe consequences of inherited defects in DDR factors resulting in various diseases, including immune deficiency, neurological degeneration, premature aging, and severe cancer susceptibility (Hoeijmakers 2009).

The involvement of DNA damage in the induction of replicative senescence by telomere erosion has been established. Activation of a DDR has also been shown to contribute to OIS in several settings *in vitro*; among others, in the context of oncogene-induced DNA hyperreplication (D'Adda di Fagagna 2008). The DDR and p53 often function in a common signal transduction cascade in which interference with specific DDR components can substitute for the loss of p53 function. However, DDR activation is not a universal feature of OIS. In line with this, senescence induced upon genetic loss of Skp2 in the context of Pten heterozygosity is not associated with the emergence of DDR markers and does not depend on p53 signaling (Lin et al. 2010). Shedding some light on a possible link between the DDR and senescence, an elegant study showed that, in the context of Rb loss-driven murine adenomas, the DDR preceded cellular senescence. While early and late adenomas similarly expressed DDR markers, senescence was apparent only in late (arrested) lesions, suggesting that, at least in this experimental system, it is primarily senescence and not DNA damage signaling that acts cytostatically. It thus seems that DDR activation is involved in certain, but not all, OIS settings (Giglia-Mari *et al.*, 2011).

Oxidative stress and senescence.

It is widely recognized that oxidative stress and ROS are strictly associated, as *in vitro* as *in vivo*. It's also largely assumed that ROS levels increase in both replicative senescence and OIS (Lee et al. 1999). ROS contribute also to induction of replicative senescence, as evidenced by its delayed or premature onset upon treatment with antioxidants or inhibitors of cellular oxidant scavengers, respectively (Chen et al. 1995; Yuan et al. 1995). A recent systems biology study has suggested that ROS mediates senescence through induction of DNA damage foci, with a contribution of p21CIP1. Passos and co-workers shown that there exists a dynamic feedback loop that is triggered by a DNA damage response (DDR) and, which after a delay of several days, locks the cell into an actively maintained state of 'deep' cellular senescence. The essential feature of the loop is that long-term activation of the checkpoint gene CDKN1A (p21) induces mitochondrial dysfunction and production of reactive oxygen species (ROS) through serial signalling through GADD45-MAPK14(p38MAPK)-GRB2-TGFBR2-TGFb. These ROS in turn replenish short-lived DNA damage foci and maintain an ongoing DDR. This loop is both necessary and sufficient for the stability of growth arrest during the establishment of the senescent phenotype. (Passos et al. 2010). Further studies try to explain how ROS relate to p53 and RB. A study on the maintenance of a senescence-like arrest upon temporary expression of SV40 LT revealed that ROS and PKC δ function in a positive feedback loop to maintain this proliferative halt. Furthermore, ROS have been suggested to impinge either directly or indirectly on the p53 and p16INK4A–RB signal transduction cascades For instance, the MINK–p38–PRAK pathway is activated in senescence and controls the activation of p16INK4A and p53, as well as expression of p21CIP1, in a p53-independent manner. These results notwithstanding, although ROS undoubtedly plays an important role in senescence, the nature and mechanism of this contribution remains largely unclear. Major questions include how the increased levels of ROS are generated, and what the cellular targets for ROS in senescence are (Kuilman et al., 2010).

Biomarkers of senescence.

Whilst cellular senescence can be induced by a wide variety of conditions, senescent cells show a number of definite features which allows their identification and that in many cases reflect the mechanism that contribute to senescence program. Cell cycle arrest is certainly the central and indispensable marker of senescence, even if it is no unique for senescent cells. In other words, terminal differentiation results in proliferative arrest.

Morphological changes accompany senescent cells which became large flat multinucleated, or refractile. As it is well known the p53 and p16^{INK4A}-RB signal transduction cascades commonly mediate the activation of the senescence program (Lowe et al. 2004). Consequently, components thereof have been used as biomarkers to identify senescent cells. In human fibroblasts undergoing replicative or premature senescence, RB accumulates in its active, hypophosphorylated form (Stein et al. 1990; Serrano et al. 1997), and p53 displays increased activity and/or levels. The p53 protein can also be phosphorylated on Ser 15 by ATM as part of the senescence response (Calabrese et al. 2009). p53 serves as a node, mediating prosenescence signals emerging from unscheduled oncogene activation, telomere dysfunction, DNA damage, and reactive oxygen species (ROS). RB has a unique role in mediating senescence in human cells, one of its primary activators, p16^{INK4A}, is commonly induced in senescent cells in many contexts in vitro (Serrano et al. 1997; Campisi 2005).

Induction of SA- β -GAL (Senescence Associated β -D-galactosidase) is a common senescence markers (Dimri et al. 1995). Its increased activity in senescent cells derives from lysosomal β -D-galactosidase, which is encoded by the GLB1 gene, however it is as yet unclear to what extent its contribute mechanistically to the senescence process.

Cellular senescence it is also associated with an altered chromatin structure, characterized by the formation of senescence associated heterochromatin foci (SAHF), nuclear DNA domains stained densely by DAPI and enriched for histone modifications including lysine9-trimethylated histone H3. SAHF contribute to senescence-associated cell growth arrest by sequestering and silencing proliferation-promoting genes such as

the E2F target gene cyclin A (Narita, et al., 2003 - 2006).

As cells approach senescence, a known chromatin regulator, HIRA, enters PML(promyelocytic leukemia) nuclear bodies, where it transiently colocalizes with HP1 proteins prior to incorporation of HP1 proteins into SAHF. A physical complex containing HIRA and another chromatin regulator, ASF1a, is rate limiting for formation of SAHF and onset of senescence, and ASF1a is required for formation of SAHF and efficient senescence-associated cell cycle exit (Zhang et al., 2005).

Cells undergoing senescence - whether in response to telomere malfunction, DNA damage, or oncogenic alterations - exhibit profound changes in their transcriptomes. A major consequence of this is the secretion of many dozens of factors, including cytokines and chemokines (Campisi 2005). The first indication of changes in the secretome of human cells accompanying senescence was reported for fibroblasts undergoing replicative senescence. Microarray expression analysis revealed a strong inflammatory response, as seen in wound healing (Shelton et al. 1999). Subsequent work from various laboratories has revealed that cells undergoing either replicative or premature senescence display profound changes in their secretome, termed the senescence-associated secretory phenotype (SASP) (Copp'e et al. 2008; ; Rodier et al. 2009). A recent study indicates that, for the induction of several of these SASP factors, persistent DNA damage is required. Because DNA damage accompanies some but not all senescence settings the SASP is not strictly coupled to senescence per se (Rodier et al. 2009).

Autophagy : between life and death.

Autophagy is an ATP- dependent mechanism highly conserved in all eukaryotic cells. Autophagy assures degradation of cytoplasmic cellular components. Autophagy process begins with an isolation membrane, also known as a phagophore that is likely derived from lipid bilayer contributed by the endoplasmic reticulum (ER) and/or the trans-Golgi and endosomes. The phagophore expands to engulf intra-cellular cargo,

such as protein aggregates, organelles and ribosomes, thereby sequestering the cargo in a double-membraned autophagosome. The loaded autophagosome matures through fusion with the lysosome, promoting the degradation of autophagosomal contents by lysosomal acid proteases. Lysosomal permeases and transporters export amino acids and other by-products of degradation back out to the cytoplasm, where they can be re-used for building macromolecules and for metabolism (Mizushima 2007).

Although the importance of autophagy is well recognized in mammalian systems, many of the mechanistic breakthroughs in delineating how autophagy is regulated and executed at the molecular level have been made in the yeast *Saccharomyces cerevisiae*. Currently, 32 different autophagy-related genes (Atg) have been identified by genetic screening in yeast and, significantly, many of these genes are conserved in slime mould, plants, worms, flies and mammals, emphasizing the importance of the autophagic process in responses to starvation across phylogeny (Nakatogawa et al., 2009).

Autophagy is a self-degradative process that is important for balancing sources of energy at critical times in development and in response to nutrient stress. Autophagy also plays a housekeeping role in removing misfolded or aggregated proteins, clearing damaged organelles, such as mitochondria, endoplasmic reticulum and peroxisomes, as well as eliminating intracellular pathogens. Thus, autophagy is generally thought of as a survival mechanism, although its deregulation has been linked to non-apoptotic cell death. In addition to elimination of intracellular aggregates and damaged organelles, autophagy promotes cellular senescence and cell surface antigen presentation, protects against genome instability and prevents necrosis, giving it a key role in preventing diseases such as cancer, neurodegeneration, cardiomyopathy, diabetes, liver disease, autoimmune diseases and infections.

Despite autophagy was first described in 1967 by De Duve, it has been rediscovered by scientist in recent years for its importance in the cell machinery, and although the growing body of findings there remain specific challenges to understanding of autophagy in mammalian cells, including how the phagophore emerges in the first place, how a specific cargo is targeted for degradation, and how

alternative mechanisms of autophagy are regulated. However, the significance of defects in autophagy for disease and ageing is apparent from growing evidence linking mutation or loss of function of key autophagy genes in cancer, neuropathy, heart disease, auto-immune disease and other conditions. From the perspective of a cancer biologist, it remains controversial whether autophagy is tumour suppressive (through cell cycle arrest, promoting genome and organelle integrity, or through inhibition of necrosis and inflammation) or oncogenic (by promoting cell survival in the face of spontaneous or induced nutrient stress). In other diseases, such as neurodegenerative diseases (Huntington's, Alzheimer's and Parkinson's diseases) and ischaemic heart disease, autophagy is more widely accepted as beneficial given its role in eliminating 'toxic assets' and promoting cell viability (Glick et al., 2010).

The mitochondrial free radical theory of aging.

In 1956, Denham Harman first proposed that the oxygen free radicals that are endogenously formed from normal metabolic processes in a variety of organisms cause aging. With accumulating evidence, and following decades of studies that have involved both invertebrate and vertebrate model systems, there is continued controversy over whether an accumulation of macromolecular damage caused by chronic ROS production limits mammalian lifespan or whether it primarily contributes to the onset of age-related disease.

Oxidatively-damaged proteins and DNA accumulate with aging. If these damages are not appropriately repaired, they can cause progressive failure of cellular machinery, organ aging and the onset of age-related disease. A number of pathologies have been linked to oxidative stress, including atherosclerosis, hypertension, ischaemia–reperfusion injury, inflammation, cystic fibrosis, diabetes, Parkinson and Alzheimer diseases, and cancer. Given that mitochondria are the major known intracellular generators of reactive oxygen species (ROS), which are the inevitable consequence of oxidative ATP production from electron transport along the mitochondrial inner membrane, this theory has largely become known as the mitochondrial free radical theory of aging.

Accepted refinements to this theory now include the chemical participation of reactive nitrogen species (RNS) as well as ROS, recognition that mitochondrial (mt)DNA damage also accumulates with aging, and appreciation that the balance of intracellular antioxidant and macromolecular repair mechanisms is crucial in determining the cell fate responses to both acute and chronic oxidative stress. It is also important to note that the free radical theory of aging is not mutually exclusive with respect to aging mechanisms illustrated above (cell senescence, telomere shortening and genomic instability).

Evidence in support of the mitochondrial free radical aging theory in mammals includes the following:

- mitochondrial ROS production and mtDNA damage (for example, deletions, mutations and base modifications) increase with age in various mammals, including mice and humans
- injection of chemically uncoupled or aged mitochondria induces cellular degeneration of knock-in mice with catalase overexpression localized to the mitochondria exhibit reduced levels of mtDNA damage and have an extended lifespan
- caloric restriction reduces mitochondrial ROS production and mtDNA damage and extends lifespan (Benz and Yau, 2008)

Cancer and neurodegeneration, an inverse relation.

Cancer and neurodegeneration are often thought of as disease mechanisms at opposite ends of a spectrum; one due to enhanced resistance to cell death and the other due to premature cell death.

Although neuronal degeneration seems to be a condition associated with aging of the organism, not all aging individuals develop neurodegeneration. There is evidence of some cognitive deterioration with aging (Levy, 1994; Rubin et al, 1998;); however the changes due to dementia are much more profound and pervasive than those associated with normal aging. Cancer, on the other hand, is a disorder that manifests itself at almost any age, but like neurodegenerative diseases, its prevalence and incidence also increase with increasing age. Both neurodegenerative diseases and cancer then, are two common and important diseases that increase with age, and lead to high morbidity and mortality in the elderly. Neurodegeneration is associated with progressive loss of neuronal cells, whereas cancer is linked with the opposite phenomenon: unregulated and increased cell survival and proliferation. Therefore, it can be hypothesized that a common biological mechanism underlies the two diseases which, when regulated in one direction leads to cell death or senescence (i.e. neurodegeneration), and when regulated in the other direction promotes cell proliferation (cancer) (Behrens et al., 2008).

There is now accumulating evidence to link so diversified processes. However, the more we learn about the molecular genetics and cell biology of cancer and neurodegeneration, the greater the overlap between these disorders appears. Many epidemiological studies have linked cancer and neurodegenerative disorders. A growing body of evidence suggests an inverse correlation between the risk of developing cancer and a neurodegenerative disorder. It has been shown that, after adjustment for age, a diagnosis of Alzheimer Disease (AD) was associated with a 60% reduced risk of cancer, and conversely a history of cancer was associated with a 30% reduced risk of AD (Bennett *et al.*,2010)

A number of studies show that the genes causing neurodegeneration are often mutated or abnormally expressed in cancer. Both cancer and neurodegeneration are thought to be the result of the interaction of genetic and environmental factors. Age is the single most important risk factor for both cancer and neurodegeneration and, although the exact cellular mechanisms of aging are not yet completely defined, age is likely to play an important role in the link between the two disorders. Both cancer and

neurodegeneration are also characterized by the contribution of the inheritance of mutated genes.

Research showing that cancer and neurodegenerative disorders share some of the same genes and molecular mechanisms strengthens the idea that individuals affected by a neurodegenerative disease may have a decreased risk of some cancers. Despite a number of intriguing pointers, little is known about the genetic association between cancer and neurodegeneration. Although a large number of genes have been implicated in the genesis of cancer and neurodegeneration, only two, *parkin* and *ATM*, have been shown to strongly overlap (Plun-Favreau *et al.*, 2010).

Further studies of the origin of both diseases indicate that their sporadic forms are the result of metabolic dysregulation and that compensatory increase in energy transduction which occurs in both diseases is inversely related. In cancer, the compensatory metabolic effect is the up-regulation of glycolysis, first described by Warburg in 1956, and known as Warburg effect; in Alzheimer Disease, a bioenergetic model based on the interaction between astrocytes and neurons indicates that the compensatory metabolic alteration is the upregulation of oxidative phosphorylation — an inverse Warburg effect. These two modes of metabolic alteration could contribute to an inverse relation between the incidence of the two diseases (Demetrius *et al.*, 2013).

Metallothioneins and oxidative stress

The thiol side chain in cysteine often participates in enzymatic reactions as a nucleophile. The thiol is susceptible to oxidization to give the disulfide derivative cystine, serves an important structural role in many proteins, such as Metallothionein (MT). MTs are small cysteine-rich metal-binding proteins found in many species and, although there are differences between them, it is of note that they have a great deal of sequence and structural homology. MT is characterized by its low molecular weight (6 to 7kDa), high metal content, characteristic amino acid composition, high content of

conserved cysteine residues and absence of aromatic amino acids. The existence of MT across species is indicative of its biological demand, while the conservation of cysteines indicates that these are undoubtedly central to the function of this protein. Over 40 years of research into MT have yielded much information on these proteins, but have failed to assign them a definitive biological role (Miles *et al*; 2000). Currently, they are considered as multifunctional proteins, playing major roles in metal detoxification and homeostatic trace element regulation, protection of cells against oxidative stress, radical scavenging, and regulation of cell proliferation and apoptosis, and the maintenance of intracellular redox balance. In mammals, predominantly Zn^{2+} , but sometimes also Cu^{2+} are bound *in vivo* under physiological conditions, but several other less abundant transition metals, such as Cd^{2+} , Bi^{3+} , Pt^{2+} , Ag^+ , and Hg^{2+} also are bound avidly by MTs. It is known that cysteines are organized into some specific cluster, as cys-x-cys, cys-x-y-cys, and cys-cys sequences. However, sometimes cysteine appear in an atypical context, cys-cys-cys or cys-x-x-cys. Cys triplets has been found to act as ligand in MTs (Serra-Batiste *et al.*,2010).

***Saccharomyces cerevisiae* as a model organism for cancer and aging**

Saccharomyces cerevisiae is a common species of yeast (Kingdom: Fungi, Phylum: Ascomycota, Subphylum: Saccharomycotina, Class: Saccharomycetes, Order: Saccharomycetales , Family: Saccharomycetaceae, Genus: Saccharomyces).

S. cerevisiae cells are generally ellipsoidal in shape ranging from 5 to 10 μm of diameter, mean cell volumes are 29 or 55 μm^3 for a haploid or a diploid cell, respectively; cell size increases with age. Yeast cells share most of the structural and functional features of higher eukaryotes, peculiarities of yeast cells are that they are surrounded by a rigid cell wall, the vacuole corresponds to lysosomes in higher cells.

S. cerevisiae is a facultative anaerobic fermenting yeast, it shows a very low Pasteur effect (inhibiting effect of oxygen on the fermentation process), and high Crabtree effect (repression of respiration, under fully aerobic conditions, in the presence of glucose).

Saccharomyces cerevisiae was the first eukaryotic genome that was completely sequenced (Goffeau et al., 1996). The genome is composed of about 12.068 kb and 6.275 genes, compactly organized on 16 chromosomes (A - P). It is estimated that yeast have at least 31% of its genes homologous with that of humans (Botstein et al., 1997).

S. cerevisiae life cycle

Although *S. cerevisiae* is a unicellular organism, it can exist in any of three specialized cell types which play distinctive roles in their life cycle. Two of the specialized cell types are the mating types α and a , which are able to mate efficiently with each other. Because the mating process results in both cell and nuclear fusion, mating produces a diploid cell. The product of mating, the zygote, has a distinctive shape and gives rise to daughter diploid cells of the usual shape by budding. It is capable of undergoing meiosis upon nutritional starvation. It gives rise to four haploid meiotic progeny, each of which is encased in a spore coat. And are wrapped up together in a sac, the ascus.

Asexual division in yeast is a process known as budding. Budding is a form of reproduction in which a new organism develops from an outgrowth or bud on another one. The new organism remains attached as it grows, separating from the parent organism only when it is mature. Since the reproduction is asexual, the newly created organism is a clone and is genetically identical to the parent organism. This process results in a 'mother' and a smaller 'daughter' cell, unlike the process of fission, in which the initial cell enlarges and then pinches off into two daughter cells. The daughter cell is a bit smaller than the mother cell and must increase in size before it initiates chromosome duplication. It is appropriate to consider the cycle as commencing with an unbudded cell in the G1 interval of the cycle. The nucleus contains a single-spindle plaque, a structure embedded in the nuclear membrane from which microtubules arise. Three events, mark the end of the G1 interval: spindle plaque duplication, the initiation of DNA synthesis, and the emergence of the bud. A diploid cell growing with adequate nutrient at the optimal temperature, 30 °C, may complete a cycle in about 100 min.

Yeast cells abandon the proliferative mode under certain environmental circumstances. For example, if they run out of nutrients, they arrest as unbudded cells in the G1 phase of the cell cycle, where they are able to survive and to resume growth when nutrients are available again. Another environmental influence that interrupts the proliferation mode is the vicinity of another yeast cell with which it can mate. If cells of different mating type are put near each other, the mating partners transiently arrest each other's cell cycle in the G1 phase and then undergo cell fusion. The mating factors cause cells to arrest in the G1 phase of the cell division cycle, just before the initiation of DNA synthesis; they are thus negative growth factors.

When a culture of yeast cells is inoculated in a fresh growth medium, a diauxic growth curve can be with three main phases (lag, exponential and stationary) can be generate (Fig.1)

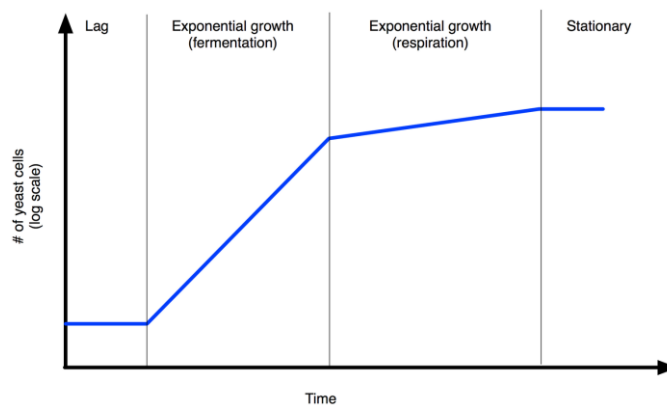


Fig. 1 Growth curve of *S. cerevisiae* culture

The lag phase refers the initial growth phase, where cells are biochemically active but non dividing, the duration and extent of this phase depends on the initial population size and environmental conditions like temperature, oxygen, nutrients etc. The exponential phase of growth is the period in which cells are actively dividing and grow most rapidly. Generally glucose is the carbon source used and fermentation is the preferential metabolic way. The third phase in growth of yeast is stationary phase when metabolism slows down and the cells stop rapid cell division. The factors that cause cells to enter stationary phase are related to change in the environment typically caused

by high cell density, nutrient starvation, or metabolic shift towards respiration. Ethanol or other carbon sources with two or three carbon atoms are used, cells produce and store trehalose and glycogen, cells become more stress resistant.

Whole nutrient absence determines the so-called long-term stationary phase, where cells do not divide, metabolism rates are lower and cells remain viable for very long time (weeks or months) without nutrient. Finally, death phase is established, so that cells die until culture lapse.

The replicative and chronological life spans are two established paradigms used to study aging in yeast. Replicative aging is defined as the number of daughter cells a single yeast mother cell produces before senescence; chronological aging is defined by the length of time cells can survive in a non-dividing, quiescence-like state.

A yeast model for aging

Saccharomyces cerevisiae is an important model organism for biological study, particularly for genetics and molecular biology. Many of the recent insights into cell cycle regulation and cancer have been achieved by using *S.cerevisiae*. Studies done over the past 50 years have led to the idea that budding yeast can be used to study three types of cellular aging. Replicative aging describes the division potential of individual cells and relies on the asymmetric cell divisions of budding yeast that yield distinct mother and daughter cells. Replicative life span (RLS) is defined as the number of times an individual cell divides before it undergoes senescence (Mortimer and Johnston 1959). Chronological lifespan (CLS) describes the capacity of cells in stationary phase (analogous to G_0 in higher eukaryotes) to maintain viability over time, which is assayed by their ability to reenter the cell cycle when nutrients are reintroduced (Longo et al. 1996). CLS has been proposed as a model for the aging of post-mitotic tissues in mammals (Wilson Powers et al., 2006).

Finally, budding yeast have been used to study clonal senescence, which is analogous to the Hayflick limit imposed on mammalian tissue culture cells and

characterized by a finite number of times a population of cells can divide. (Lindstrom *et al.*, 2009).

Genome-wide comparative RNA profiling with selected cellular model systems of aging, including replicative senescence, stress-induced premature senescence, and distinct other forms of cellular aging, allowed the identification of new genetic regulators of cellular aging and senescence, including a number of genes and pathways not previously been linked to aging. An unbiased screen across species uncovered several so far unrecognized molecular pathways for cellular aging that are conserved in evolution. Both upregulated and downregulated genes were considered. Starting with a total of 6750 human genes, 553 yeast orthologs were identified, of which only the nonessential genes were considered for further analysis (Laschober *et al.*, 2010).

For the top ranking human genes, 93 nonessential yeast orthologs were identified. Several candidate genes obtained through this analysis have been confirmed by functional experiments. The effect of genetic deletion on chronological lifespan in yeast was assessed for 93 genes whose functional homologues were found in the yeast genome and the deletion strain was viable.

Several genes whose deletion led to significant changes of chronological lifespan in yeast were identified featuring both lifespan shortening and lifespan extension. The ability of a particular gene to restrict lifespan in yeast suggests it plays a role in modulating the rate of aging that potentially extends beyond yeast.

The Region of Minimal Deletion on chromosome 6q26-27.

In past years, a relationship between the establishment of a senescence phenotype and 6q region was demonstrated. Sandhu and co-workers showed that introduction of a normal human chromosome 6 or 6q - by microcell-mediated chromosome transfer (MMCT) - can suppress the immortal phenotype of simian virus 40-transformed human fibroblasts (SV/HF). At least one of the genes for cellular

senescence in human fibroblasts should be present on the long arm of chromosome 6 (Sandhu, 1994).

Cytogenetic and molecular studies showed 6q26-27 chromosome rearrangement involved in some different type of cancer, such as ovarian cancer (Trent, 1980; Tibiletti, et al., 1998), breast cancer (Negrini et al, 1994), gastric carcinoma (Carvalho, et al., 2001), chronic lymphocytic leukemia (Amiel, et al., 1999), B-cell non-Hodgkin lymphoma (Gaidano, 1992), and others.

To define a small region on chromosome 6q containing a putative tumor suppressor gene for ovarian cancer, 70 ovarian tumors of three histological types were scored for loss of heterozygosity with nine restriction fragment length polymorphism markers located at 6q24-27. The results supported earlier suggestion that alteration of a gene on chromosome 6q may play an important role during development of serous ovarian tumors (Saito et al., 1992).

A detailed deletion map indicated a commonly deleted region between D6S193 e D6S149 loci; these markers were estimated to be 1.9 cM apart (Saito, 1992), but this distance was reduced to about 700-800 kb by physical mapping methods. Within this Region of Minimal Deletion (RMD) one or more tumor suppressor genes should be present.

Banga and co-workers showed that SV40-immortalized fibroblast cell lines share a deletion in this area based on assessment for loss of heterozygosity (LOH) for seven informative markers on 6q. They suggested the presence of a senescence locus, called SEN6, on 6q27. Inactivation of SEN6 may be responsible for immortalization of these tumors (Banga, et al, 1997). SEN6 overlaps to RMD. The genetic locus of the putative tumor suppressor gene was better delineated by Lin and Morin, who found an 80 kb homozygous deletion (HD) encompassing marker D6S193 (Fig.2) at 6q27 in a ovarian cancer cell lines (Lin and Morin, 2001).

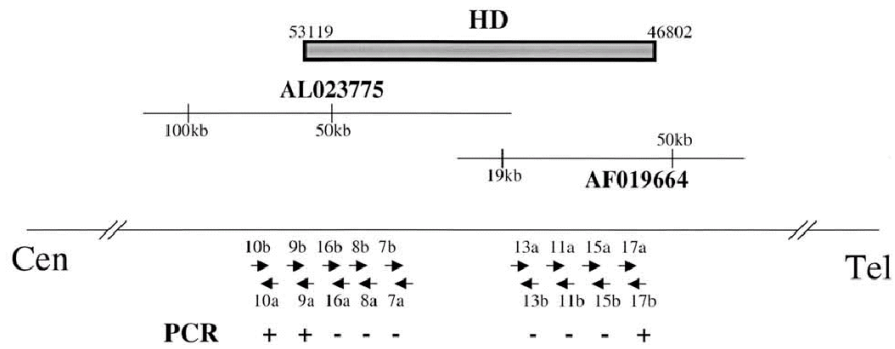


Fig. 2 Contig of the HD region (from Lin and Morin, 2001).

The catp gene.

Our study began with the project “Genetica Molecolare del processo di senescenza” at IRCSS Oasi Maria SS. - Troina (EN). The aim of this study was to identify genes present on 6q27 region.

By “direct cDNA selection” (Lovett, 1991), an EST was identified mapping to the RMD. It was present as single copy and contains a short open reading frame (360 bp) without introns. Analysis for this new putative gene began with bioinformatics searches; however, nucleotide and protein Blast against sequence databases did not show any homology with known sequences, either nucleotidic or aminoacidic. For this gene the transitional name catp (Cytomembrane Associated Trafficking Protein) was chosen because bioinformatics analysis predicted the presence of a cytomembrane binding domain to its C-terminus. The EST has been deposited on GenBank with accession number AF453446.

Chapter 2

IDENTIFICATION OF A NOVEL GENE

RESULTS

Direct cDNA selection: identification of a cDNA mapping to 6q26 region.

The RMD at 6q27 was the starting point of this study. A “direct cDNA selection” approach (Lovett, 1991) was devised in order to enrich and isolate individual cDNAs mapping to that chromosomal region, through hybridation of a fetal brain cDNA library versus genomic clones. mRNA composition in fetal brain is estimated to represent up to 70% of the genomic information. In order to identify genes present on 6q27, the YAC 911C10 was choiced since it mapped precisely on the region of interest (Fig.3), and subcloned in cosmids.

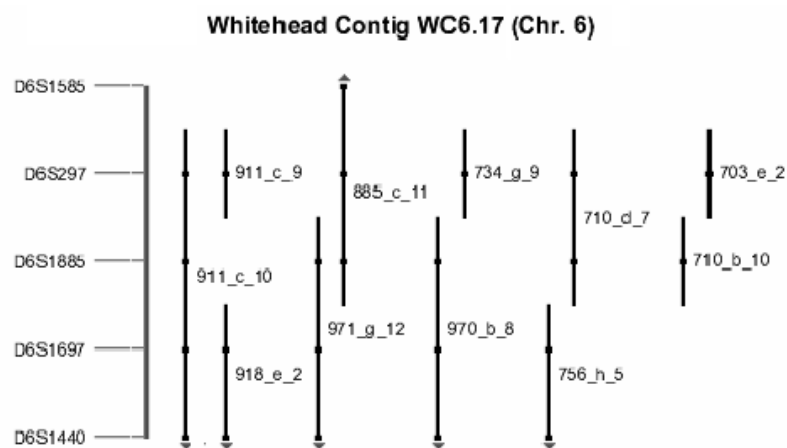


Fig. 3 3YAC contig map encompassing the critical region of the RMD

Inserts were rescued by PCR amplification with specific primers by nested PCR. The cDNA:DNA hybrids which resisted to high stringency washes were recovered by denaturation and PCR re-amplified. The cDNAs pool obtained was tested through Southern blot and dot blot both on YAC 911C10 and cosmids derived from it (Fig.4). All these data together suggest that at least one of the selected cDNA gave a prominent band on Southern blot and thus match the 6q27 region. The enriched cDNAs were finally cloned in pUC18 vectors and transformed in DH5 α host.

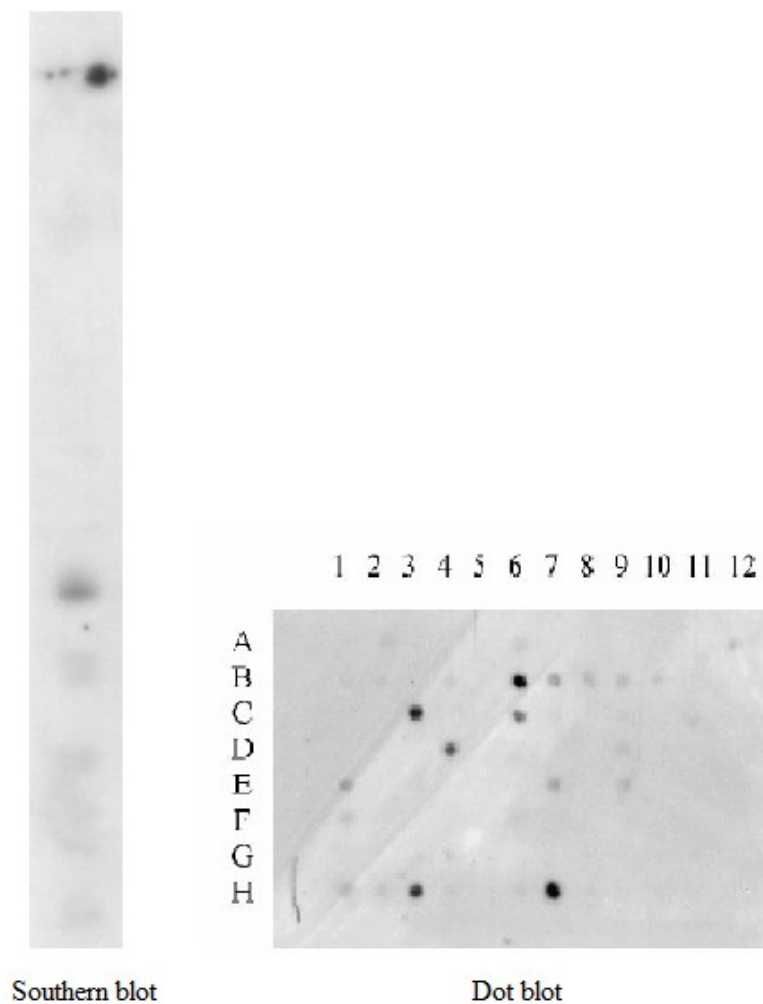


Fig. 4 Southern blot analysis of YAC911C10 and Dot blot of derived cosmids.

A clone encompassing a 700 bp fragment was isolated, extracted, sequenced and subjected to bioinformatics analysis. Blastn versus genomic databases revealed that it matches BACs mapping to 6q26-27, while no match was seen against any EST library. This cDNA was then submitted to GenBank (AF453446). Overall, the data obtained suggest that this cDNA indeed mapped to 6q27, was present as single copy and was possibly a novel gene.

A single ORF 363 bp long was found within the cDNA sequence.

***catp* expression.**

After identification of the gene, studying its expression was the first step to confirm its transcription in brain cells. RT-PCR experiments on cell lines of neuroblastoma and glioma origin, revealed the presence of *catp* transcripts, even if at low levels. Neuroblastoma SH-SY5Y line gave more consistent results (Fig.5).

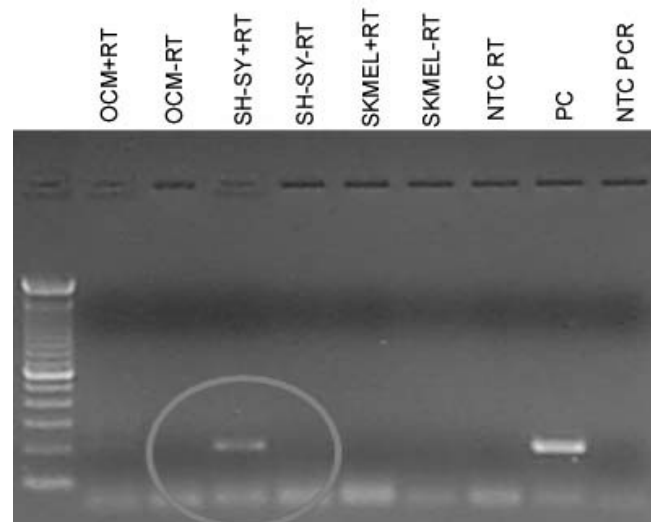


Fig. 5 RT_PCR on human cell lines.

Mutational analysis.

The presence of *catp* within the RMD raises the question about its implication in tumors. Genes implicated in cancer, either sporadic or familial, often present mutations, either somatic or germline. The relevance of single point mutations for this argument led us to investigate for the presence of mutations on this gene.

One germline mutation was found in a preliminary screening of normal population from Sicily. It consisted in a point mutation causing Arg12 changing to Trp. Wild-type allele was called Up1 and the mutant UpB. The allelic frequency are 94% and 6% respectively. When cloned into pET expression vector in *E.coli*, alleles showed different growth properties. The wild type grew poorly and showed a phenotype compatible with oxidative stress. That plasmid was occasionally rearranged in culture; on the other hand, the mutant (UpB) did not show any problem in growth and DNA or protein syntheses were normal. Since alleles differ only by one point mutation, differences in growth ability appeared of some relevance. Further assays suggested that the difficult growth of the wild type allele was possibly due to Iron starvation, since growth was restored following addition of Fe citrate.

This consideration encouraged me to investigate for the presence of further mutations on this gene. SNPs are described in bioinformatics databases dbSNP short genetic variations (<http://www.ncbi.nlm.nih.gov/snp/>). Five SNPs are known to map within *catp* sequence (Fig.6).

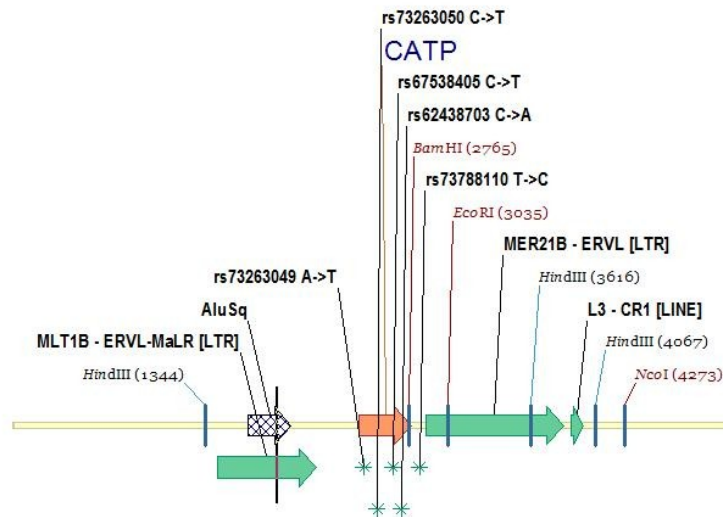


Fig. 6 SNPs mapped to *catp* sequence.

In order to evaluate the presence of those variations in human population, we made use of DHPLC, a powerful techniques for identifying point mutations, to screen a sample of an African population from Burkina Faso. Four different heterozygote profiles were found (Fig.7). DNA from individuals belonging of each group was sequenced and three of the aforementioned SNPs were identified. One of them, rs73263049, represented the same c.34A>T transversion already found in Sicily; rs73263050 was found to create a missense mutation c.127C>T, causing Arg43 changing to Cys, and rs67538405 a nonsense mutation c.238C>T.

Those mutations were found arranged in four different genotypes, indicated in Table I as heterozygous groups.

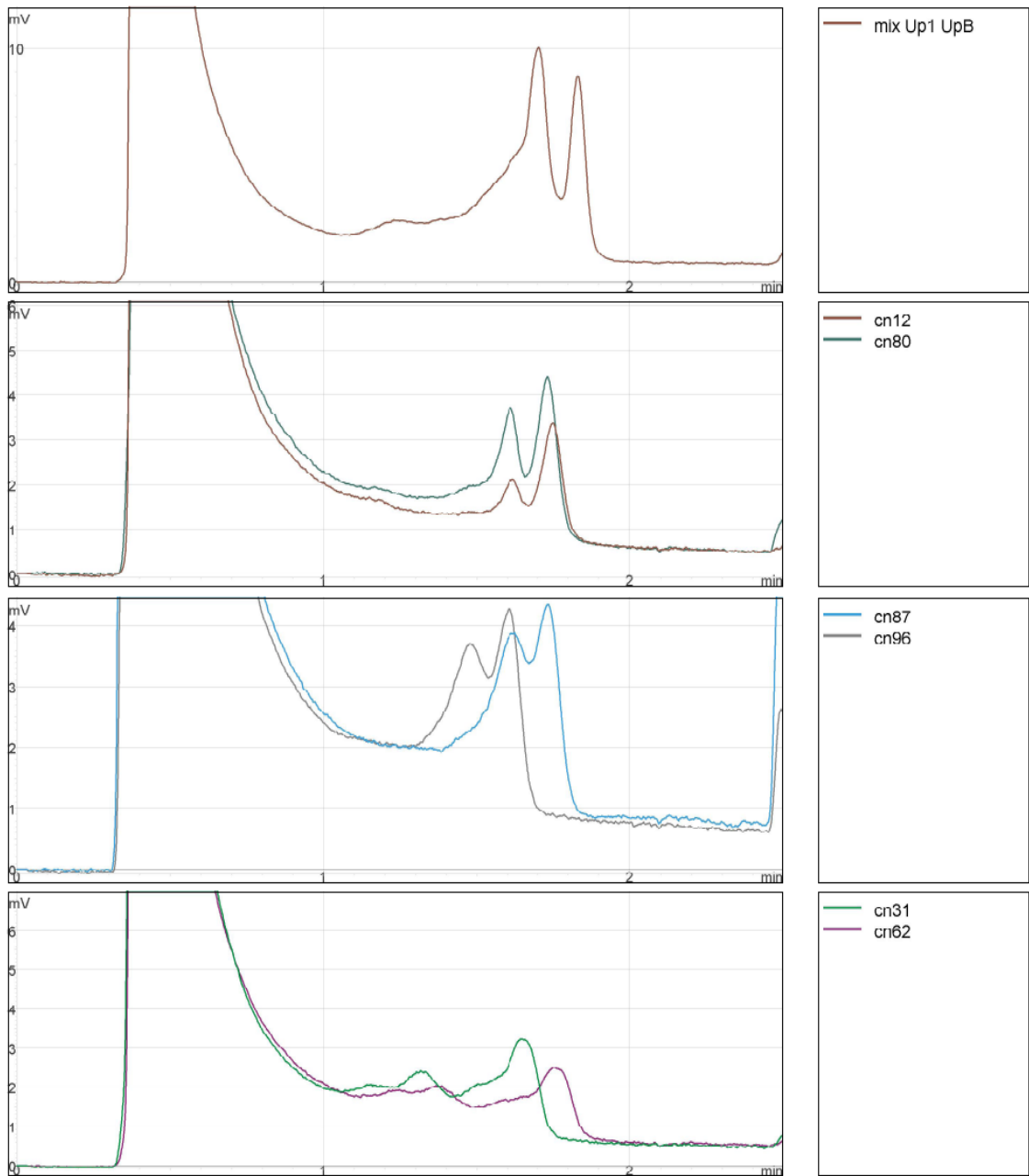


Fig. 7 DHPLC profiles

	c.34A>T	c.127C>T	c.238C>T	SNP	codon	aminoacid
hetero1	x			c.34A>T	AGG → TGG	R12W
hetero2	x	x	x	c.127C>T	CGC → TGC	R43C
hetero3	x		x	c.238C>T	CAG → TAG	Q80STOP
hetero5			x			
heterozygous groups				mutations		

Tab I Collections of mutants in human sample population from Burkina Faso.

Establishing the phase, i.e. the ways the mutation are arranged into alleles, was my next goal. To this purpose, I cloned PCR products in *E.coli*. Each plasmid now carried only one allele, so by sequencing I could establish the precise association (*cis* or *trans*) of mutations in those alleles. Surprisingly, all multiple mutations were found in *cis* arrangement. Allelic frequency for wild-type allele was about the same both in Sicilian and in African population samples, whereas lower frequencies were found for the other ones. Data collected allowed to define overall five alleles for the gene *catp*. Genotypes are showed in table II.

Allele name	Genotype	SNP #	Aa substitution	Allele frequency(%)
Up1	wt	-	-	94
UpB	c.34A>T	rs73263049	R12W	6 (Sicily) 3 (Burkina Faso)
Trunk	c.238C>T	rs67538405	Q80STOP	1 (Burkina Faso)
Double	c.34A>T c.127C>T	rs73263049 rs73263050	R12W R43C	1 (Burkina Faso)
Triple	c.34A>T c.238C>T c.127C>T	rs73263049 rs73263050 rs67538405	R12W R43C Q80STOP	1 (Burkina Faso)

Tab II *catp* alleles: genotypes and allele frequencies.

Evolution.

Another way for analyzing the function of *capt* was comparing its sequence with those of Great Apes. Recent advances in genomic sequencing of Great Apes such as *Pan troglodytes* (chimpanzee) and *Gorilla gorilla* (gorilla), allowed to recognize a detailed model of molecular evolution for Higher Primates.

I was motivated to achieve a multialignment between human, chimpanzee and gorilla. The gorilla assembly was included with human chimpanzee and macaque in a 5-way whole genome alignment using the Ensembl EPO pipeline⁶. Using the UCSC genome browser and Ensembl, I was able to search and analyse the region of my interest in each species of interest. A multiple alignment was obtained with gorilla and chimpanzee sequences in the region corresponding to *catp* gene and flanking sequences (human chr6:167,078,690-167,080,192; chimpanzee chr6:169,870,326-169,872,575; gorilla chr6:168,084,094-168,543,716). Sequences from *Homo neandertalensis* and *H. denisovian* were omitted, since they were fully coincident with that of *Homo sapiens sapiens*; similarly, the sequence of orangutang were also omitted because it was found to be more divergent.

Multiple alignment shows high similarity among all sequences isolated. All of them presented a sequence high homologous with *catp*; so my attention was focused on variations within CDS (Fig.8). Three synonymous variations and four missense substitution were found; while nucleotide substitutions found in gorilla sequence are in some cases common to chimpanzee, a few other are peculiar of the former species. In particular, five sites, mutated in chimpanzee, are common in gorilla and in human; two synonymous substitution and five substitutions resulting in amino acid change occur only in gorilla; one synonymous and two amino acid substitution are common to chimpanzee and gorilla sequences. One of them, a first position transition 79C>T, seems more interesting because it introduces a Arg to Cys mutation; since this is followed by two consecutive Cys, a Cys triplet forms in human protein which is absent in Great Apes. Cys triplets are rare in protein databases (about 50 entries on 8 millions), especially in higher Vertebrates. Thus, one could believe that this mutation may constitute a *gain of function* in human compared to Great Apes. I did some preliminary experiments in order to test this hypothesis (see funcional analysis in yeast model).

```

est9      AAATAGAGACTAATTTGGAAAAGAGCTGTCAGGCCCAACAGAATATTAATGTTGCTGCTG
human     AAATAGAGACTAATTTGGAAAAGAGCTGTCAGGCCCaACAGAATATTAATGtTGCTGCTG
chimp     AAATAGAGACTAATTTGGAAAAGAGCTGTCAGGCCcgACAGAATATTAATGgTGCTGCTG
gorgor    AAATAGAGACTAATTTGGAAAAGAGCTGTCAGGCCCAGACAGAATATTAATGGTGTGCTG
*****.*****

est9      TGGTTGCCcAGTGAGGACATGAGGAACGAAACACAGAACATCACTCGCTCACATCTGAGC 34A>T
human     TGGTTGCCcAGTGAGGACATGAGGAACGAAACACAGAACATCACTcGCTCACATCTGAGC
chimp     TGGTTGCCcAGTGAGGACATGAGGAACGAAACACAGAACATCACgtGCTCACATCTGAGC
gorgor    CGGTTGCCcAGGAGGACATGAGGAACGAAACACAGAACATCACTCGCTCACATCTGAGC
*****

est9      CAGCGGtGCTGCTGTGAGTCTCTAAGAAGTATCCGTGTTGCAGCTACTGAGACACGCTTT 127C>T
human     CAGCGGtGCTGCTGTGAGTCTCTAAGAAGTATCCGTGTTGCAGCTACTGAGACACGCTTT
chimp     CAGCGGcGCTGCTGTGAGTCTCTAAGAAGTATCCGTGTTGCAGCTACTGAGACACGCTTT
gorgor    CAGCGGcGCTGCTGTGAGTCTCTAAGAAGTATCCGTGTTGCAGCTACTGAGACACGCTTT 79C>T
*****

est9      TTCTGCCCgGGTCACCTTCCGCCTCTACAGATTCTTTAGATGGTCCTTTcAGCAAAGA
human     TTCTGCCCgGGTCACCTTCCgCCTCTACAGATTCTTTAGATGGTCCTTTcAGCAAAGA
chimp     TTCTGCCCtGGGTCACCTTCCaCCTCTACAGATTCTTTAGATGGTCCTTTcAGCAAAGA
gorgor    TTCTGCCCgGGTCACCTTCTGCCTCTACAGATATCTTTAGATGGTCCTTTcAGCAAAGA
*****.*****

est9      AGCCAGTGGACAGCTGAGTGGCCAGTGCCTTGGGACGCACACCCAGCTGGAGTATGCA 238A>T
human     AGCCAGTGGACAGCTGAGTGGCCAGTGCCTTGGGACGCACACCCAGCTGGAGTATGcA
chimp     AGCCAGTGGACAGCTGAGTGGCCAGTGCCTTGGGACGCACACCCAGCTGGAGTATGtA
gorgor    AGCCAGTGGACAGCTGAGTGGCCAGTGCCTTGGGACACACACCCAGCTGGAGTATGCA
*****

est9      GGCTCTCCCAGAGCAGGCAAGGCCATGTGATAAGAACAACCCGAGCTTTcCTCTGAGC
human     GGCTCTCCCAGAGCAGGCAAGGCCATGTGATAAGAACAACCCGAGcTTTcCTCTGAGC
chimp     GGCTCTCCCAGAGCAGGCAAGGCCATGTGATAAGAACAACCCGAGtTTTcCTCTGAGC
gorgor    GGCTCTCCCAGAGCAGGCAAGACCATGTGATAAGAACAACCCGAGTTTTcCTCTGAGC
*****.*****

```

Fig. 8 - Multiple alignment of *catp* sequence in primate. The point mutation giving rise to a Cys triplet in human is highlighted (yellow)

Distribution of *catp* alleles in human pathologies

Next goal was to investigate distribution of wild type and c.34A>T mutation (rs73263049) - the most recurrent among *catp* polymorphisms - in genomic DNA of different pathological samples.

Since the inverse association between cancer and neurodegenerative disorder, we analyzed patients affected by neurological disorder, such as Alzheimer Disease (AD), and others, and by cancers, particularly we addressed our analysis to myeloid leukemias (ML) since some level of expression of the region of our interest was detected in K562 cells, i.e. the first human immortalised myelogenous leukemia line (USCS genome browser data).

Custom SNP Genotyping Assay was designed (Applied Biosystems®) by submitting target region encompassing rs73263049 SNP, for Real-Time PCR SNP Genotyping experiments. Examples of fluoresce curve (Fig.9) obtained (StepOne™ Software) were shown for two heterozygous compared to amplicons of known alleles, used as positive controls.

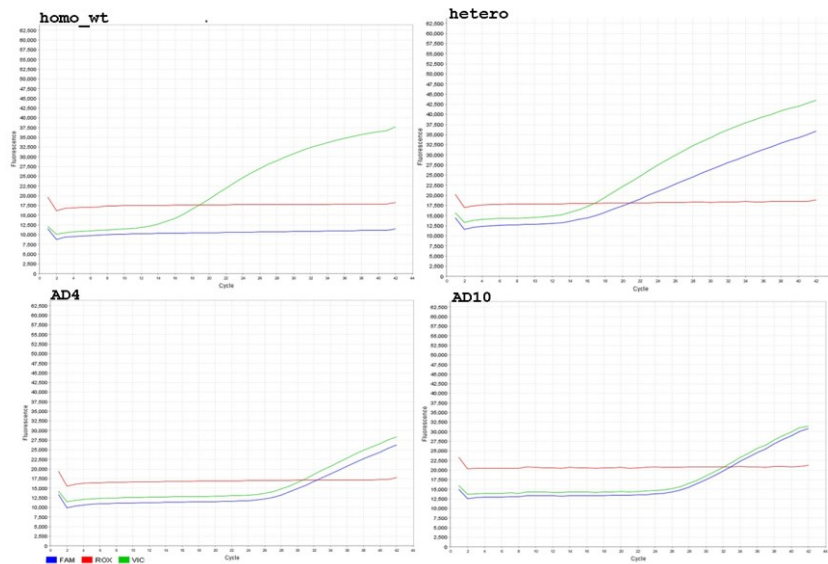


Fig. 9 c.34A>T SNP assay fluoresce curves.

Allelic Discrimination Plot (Fig.10) was generated by dedicated Applied Biosystems® TaqMan® Genotyper Software: heterozygous samples found clustered with positive heterozygous control (green), while all wt-homozygous clustered together (red).

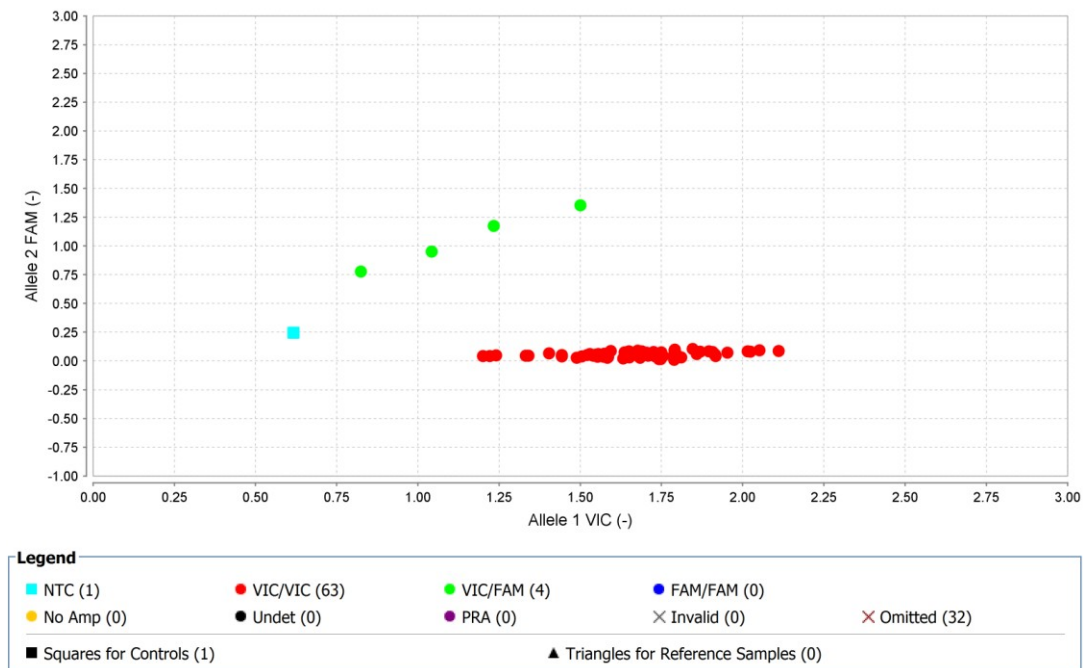


Fig. 10 Allelic Discrimination Plot example (TaqMan® Genotyper Software). Four AD heterozygous are shown.

Data so far collected are summarized in Table III; according to expected for low frequent allele, any c.34A>T homozygous and few heterozygous were found, however cohort's sizes are still too small for obtaining statistically significant results.

	tot	homo wt	hetero	homo 34A>T	alleles tot	allele wt	allele 34T	Minor Allele frequency
Neurodisorder								
AD	85	78	7	/	170	163	7	4.12%
EIEE	15	13	2	/	30	28	2	6.67%
ASD	12	12	0	/	24	24	0	0.00%
Cancers								
AML	34	32	2	/	68	66	2	2.94%
CML	9	8	1	/	18	17	1	5.56%
ML tot	43	40	3	/	86	83	3	3.49%
Melanoma	4	4	0	/	8	8	0	0.00%
Tot	202	187	15	/	404	389	15	3.71%

Tab III wild type and c.34A>T variant distribution in different pathological conditions.

A sample of 85 patients with clinical diagnosis of Alzheimer Disease (AD) was the widest group analyzed, Minor Allele Frequency (MAF) in AD found is 4.12%, c.34A>T seems to be slightly, although not significantly, hypo-represented. MAF calculated for Acute Myeloid Leukemia (AML) is even lower (2.94%).

I have also tested Autism Spectrum Disorder (ASD), which however, did not show any heterozygotes.

A cohort of children affected by Early Infantile Epileptic Encephalopathy (EIEE) with Intellectual Disability (ID) was investigated. Among them two heterozygotes were found: clinical diagnosis of acute ID and symptomatic partial epilepsy (time of first critical episode 9 months) and hypothyroidism; West Syndrome (spasms, psychomotor impairment and EEG hypsarrhythmia) are their clinical diagnosis. We know that both ASD and EIEE are complex multifactorial conditions, this, together with the small number of patients, makes data not totally meaningful. The same consideration can be extended to others tumor groups assayed: Chronic Myeloid Leukemia (CML) and Melanoma which count too little cases analyzed in our study.

I can conclude that although SNP c.34A>T frequency seems to be only slightly divergent with respect to normal population, the sample size of pathological samples is not adequate for obtaining statistical significance, especially when dealing with skewed allele distribution such that involving wt / c.34A>T. Further increase in sample size of pathological will be necessary to draw more exhaustive conclusion.

DISCUSSION

Evidences of *catp* as a novel gene

The gene *catp* could have been so elusive as to escape massive searches for genes, both bioinformatic and experimental (EST libraries), for several reasons. The first reason consists in its sequence, which is unique. One more reason is that its expression level is apparently very low, at least in fetal brain. Moreover, it falls between two highly repetitive sequences, one of which (*Alu*) is possibly transcribed. It is known that automated removal of repetitive sequences was programmed in most, if not all, EST sequencing software. Finally, it presents a unique exon, while the most widely used softwares for gene identification mainly relies on intron-exon junction finding.

The results of my study allow to draw at least some conclusions. The frequency of the more abundant allele is about the same in Sicily and Burkina Faso; for this reason I assume it is the 'normal' allele; moreover, it is present in Neanderthal's and Denisov's sequences. An orthologous sequence with some point mutations is found in chimpanzee and gorilla. Amino acid substitution rate reflects the average of gene coding variations found in whole chimpanzee and gorilla genomes (The Chimpanzee sequencing and analysis consortium, 2005; Scally et al., 2012). Thus, *catp* gene could have evolved from a sequence common in Great Apes (both gorilla and chimpanzee) through a C->T transition, which in turn led to the substitution of the 28th amino acid, Arg, with Cys. As a consequence, the peptide *ArgArgCysCys* gave rise to *ArgCysCysCys*, so that a very unusual Cys triplet was formed. In fact, screening the complete protein databases (including viruses, plants, bacteria etc.) allowed to find only about 50 Cys triplets on over 8 million proteins.

A key hypothesis of my study is that this amino acid replacement led to a gain of function, and this possibility was addressed by functional analysis in yeast (see below). However, a further consideration should be discussed here. Let us assume that *catp* originated from a 'silent' DNA segment through the occurring of a mutation; however, one may wonder that a functional protein may arise in such a way. In fact, most, if not

all, proteins known have been shaped by evolutionary processes during millions years. The discovery of several alleles – apart from the wild type – in African population shows that some evolution of *catp* indeed occurred. Two point mutations, c.34A>T and c.238C>T, should have been independently originated; but at least one recombination event should be invoked in order to explain the formation of double and triple mutants (see Table II). Since this occurred on a DNA segment <300 bp long, a strong selective pressure, presumably against the c.34A>T allele, has to be postulated. Similar recombination frequencies, which are common in bacterial genetics, are quite unusual in human genome.

Analysing the alleles' distribution in two different groups of patients, including those suffering from brain-related diseases (epilepsy, autism, and Alzheimer diseases) and from leukemia, however, showed only slightly, not significant alterations in allele frequencies were found. It is possible, however, that much larger cohorts of patients should be recruited in order to get significant results.

Chapter 3

CATP PROTEIN

RESULTS

Bioinformatic predictions of *CATP* structure.

The *catp* gene contains a short open reading frame (360 bp) without introns, coding for a 121aa-long protein. Functional analysis of unknown proteins could be facilitated by homology studies by comparison with database of known genes or proteins, or secondary / tertiary structure prediction. Since *CATP* doesn't shows any homology with known protein sequences, bioinformatics analysis was used to decipher some of the protein features through PROSITE on line tool (<http://prosite.expasy.org>). Secondary structure and disorder prediction obtained by InterproScan (Zdobnov *et al.*, 2001) indicates the presence of a α -helix domain to its N-end (Fig.11). The remaining, including the C-terminus, was organized as coiled-coil, with the exception of two segments, located at residues 2-5 and 41-45, showing high scores for beta strand.

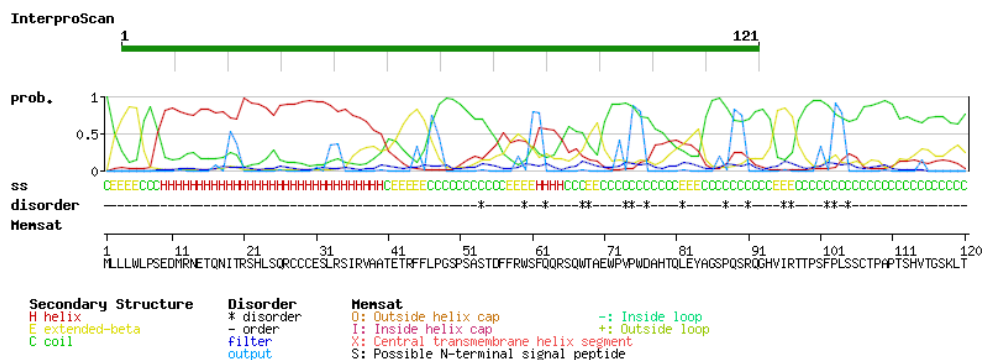


Fig. 11 Secondary Structure prediction obtained by InterproScan.

by intracardiac perfusion, in agreement with national and local legislations regulating animal health care. Sera were checked by dot blot analysis for affinity towards the peptide before use in immunoassay. For monoclonal antibody production, the same peptide was sent to Inbiolabs (Tallinn, Estonia), a biotec company specialized in immune research, in order to make hybridomas. Five of them (4A7, 2G1, 5C6, 8A2, G1) which gave positive results were inoculated in mice in order to produce ascites. 6 to 14 mg crude IgG (subtype G1) were obtained for each hybridoma.

Immunohistochemistry

Studies of *CATP* protein began with the identification of the hypothetical protein in normal and pathological human tissues by producing polyclonal antibodies in the laboratory. In particular, two kinds of antibodies were produced: antibodies against a recombinant protein obtained in *E. coli*, and antibodies against a synthetic peptide. However, antibodies obtained from the recombinant protein gave more intense background than those developed against the synthetic peptide and were discarded.

Slides with normal and pathological human tissues were obtained from Anatomopathology Unit of Cannizzaro Hospital (Catania) as paraffin-embedded 5 μ m slices. Slides were then pre-incubated with 3% bovine serum albumin (BSA) in TBS for 30 min, incubated with 1 : 200 dilution of the antibody in TBS containing 1% BSA, thoroughly washed in washing buffer before revelation with the LSAB 2 kit (anti-mouse, biotinylated and peroxidase-labelled streptavidin) and 3,3'-diaminobenzidine-4HCl (DAB; Dako, Carpinteria CA, USA) from Dako.

Immunohistochemistry on different normal and pathological human tissues gave different results. Uterine epithelium tested resulted negative, whereas positive signals were obtained from breast adenocarcinoma and from normal gastric mucosa (Fig.13).

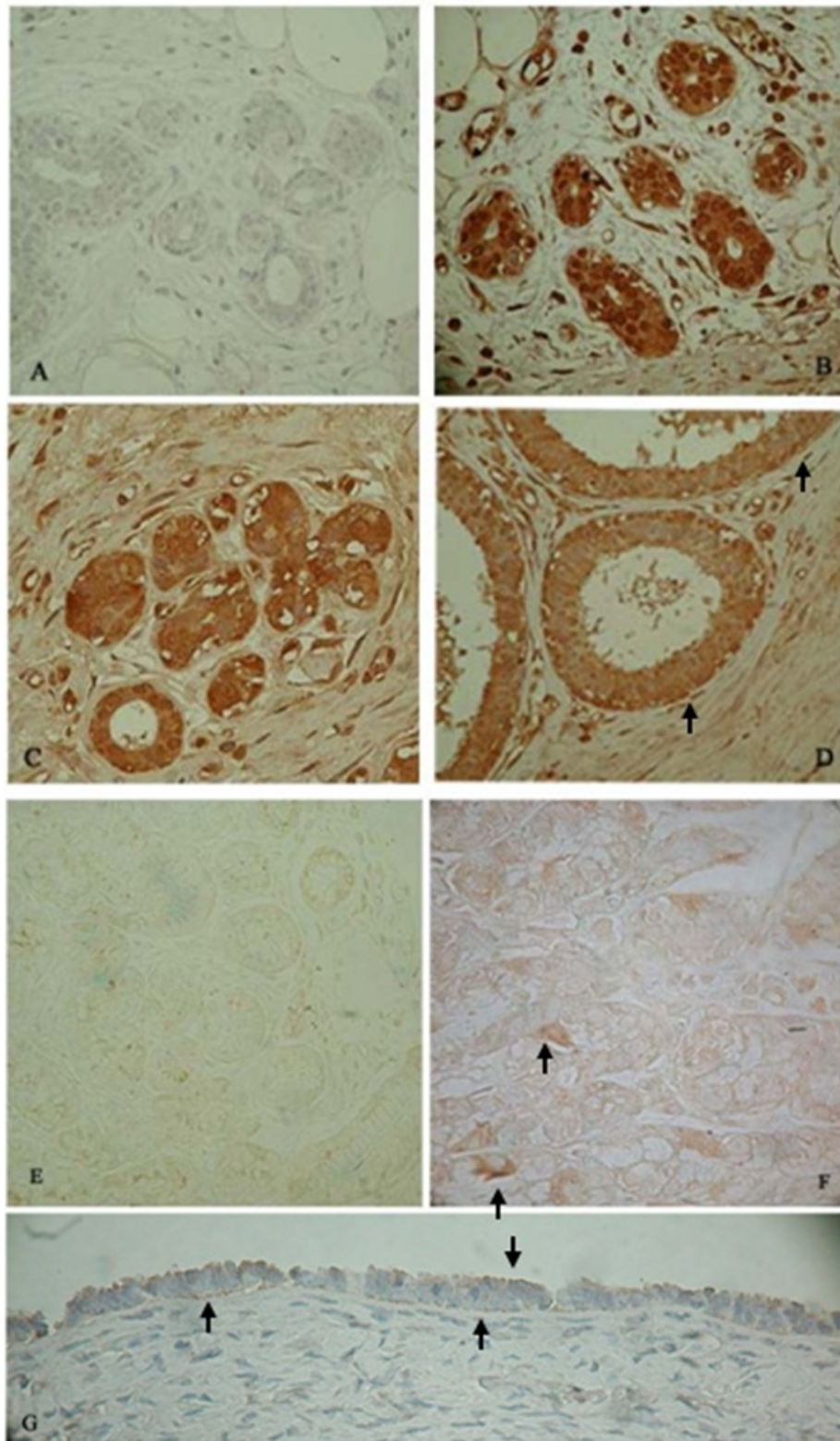


Fig. 13 Mammary carcinoma with pre-immune serum (A); anti-recombinant protein serum (B); anti-peptide serum (C,D). Anti-peptide serum shows better discrimination and lower background than anti-recombinant protein serum. Normal gastric mucosa probed with pre-immune serum (E) and anti peptide serum (F). Normal ovarian epithelium stained with anti-peptide serum (G). Note that antibody decorates the basal lamina as well as the apical (secerning) region of epithelial cells.

Immunofluorescence.

SH-SY5Y cells seeded on 4-well Lab-Tek™ II Chamber Slide™ System (Nunc Nunc International Corporation, Naperville, IL). Cells were incubated overnight with a cocktail of 5 monoclonal antibodies in 10% FBS. Cells were rinsed three times with PBS and incubated for 3 h with 488 Alexa anti-mouse IgG secondary antibody in 5% FBS. Cells were visualized using a Nikon Diaphot 200 epifluorescence microscope and a Digital Spot CCD camera (Diagnostic Instruments) was used to capture images.

Monoclonal antibodies were assayed by direct immunofluorescence on SH-SY5Y neuroblastoma cells (Fig. 14).

Taken together, results allowed to speculate about a cytoplasmic protein, expressed especially in epithelial tissues, even if at low level. Importantly, both immunohistochemical and immunofluorescence data agree about the cytolocalization. Staining of basal membrane is seen in ovaric epithelium, in normal ducts on mammary gland and in some of the SH-SY5Y cells. Additionally, in most dividing neuroblastoma cells signals clustered within a paranuclear cytoplasmic region which presumably contains the ergastoplasmic reticulum; in those cells which present cytoplasmic dendritic- or axon-like projections, discrete signals were seen. Finally, some vacuoles are stained by the antibody.

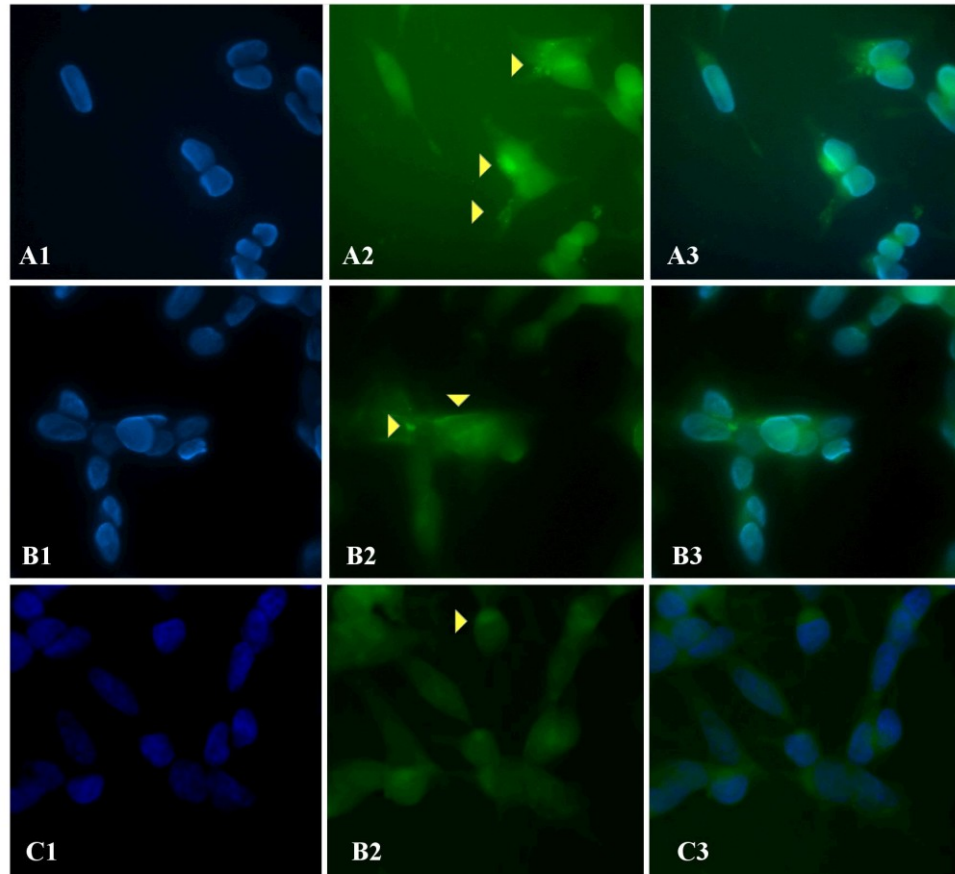


Fig. 14 CATP cytolocalization by immuofluorescence in SH-SY5Y cells by a cocktail of monoclonal antibodies. Three different fields (A, B, C) are shown. 1: DAPI staining; 2: antibody staining; 3: merged images

DISCUSSION

Evidences of *catp* expression were required after its identification. They were achieved by RT-PCR and immunological assays, which allowed verifying transcription of the gene into mRNA and translation as protein. Apart from genetic analysis, preliminary insights about *CATP* protein are important too for the functional analysis of this gene.

Data obtained until now support the hypothesis that *CATP* is a cytoplasmic protein, surely expressed in epithelial tissues and distributed into the cytoplasm in association with cytomembranes (ergastoplasmic reticulum, basal membrane, vacuoles). Even if these observations should be confirmed by additional evidences and more complex analysis of its cellular fate, I conclude that *CATP* is indeed expressed in at least some tissues and its cytolocalization agrees with the properties postulated on bioinformatic predictions.

Chapter 4

FUNCTIONAL ANALYSIS IN YEAST MODEL

RESULTS

Cloning

Cloning each of the alleles into an yeast expression vector was hard-working and was achieved for four alleles (wild-type, c.34A>T mutant, c.34A>T c.127C>T c.238C>T mutant and c.238C>T mutant), while I'm still trying to obtain c.34A>T c.238C>T allele construct. The constructs obtained by ligating *catp* ORF were transformed into bacteria first, its sequence verified and finally put into yeasts. Empty vector was also transformed and strain so obtained, named pRS, was used as negative control in all experimental setting.

Site-specific mutagenesis: recreating the *chimp* allele

Site-Specific mutagenesis was performed in order to create a specific substitution in the wild-type sequence to achieve the 79T>C substitution and thus a Cys-triplet lacking allele, that I named *chimp*-allele. Mutagenesis was performed through bridged-PCR with primers carrying the substitution of our interest, in order to create two complementary amplicons which are then merged with the use of external primer pairs. PCR product was cloned into plasmid vector pRS415, and sequencing confirmed the success of mutagenesis. The construct obtained was transformed into bacteria first and then into yeast host.

The chimp-transformed yeast strain experimented lot of difficulties in growing, both on broth and on agar medium (Fig.15). This didn't allow to perform some of the planned experiments.

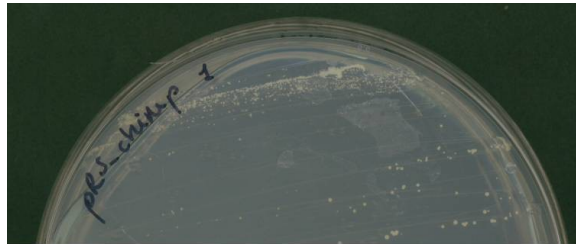


Fig. 15 chimp allele transformed yeast.

Colony morphology of yeast strains harboring *catp* alleles.

We know that metabolic conditions of cell affect yeast colony shape. Yeast colonies display a complex physiology because functional differentiation can be observed between cells of the central regions from those at the colony's edge. Metabolic, growth and death rates also differ among cells from different regions of the whole colony. Metabolic conditions deeply influences colony morphology since a multicellular colony growing on solid agar possesses several traits that are absent in individual yeast cells. These include the ability to synchronize colony population development and adapt its metabolism to different environmental changes, such as nutrient depletion. Together with cell diversification to cell variants with distinct metabolic and other properties, this contributes to the main goal of the colony population: to achieve longevity. In this respect, a benefit to individual cells is subordinated to the benefit to the whole population, exhibiting a kind of altruistic behaviour. For example, some colony cells located at particular positions undergo regulated cell dying and provide components to other cells located in more favorable areas (Váchová and Palková, 2011).

Baker's yeast forms smooth round colonies when grown in favorable conditions. When starved for one or more nutrients, yeast can alter its growth pattern to produce complex structures consisting of numerous interacting cells. One mode of growth, the

colony morphology response, produces visually striking, lacy colony architectures; fermentable carbon source limitation plus abundant nitrogen source are the key nutritional signals for inducing complex colony morphology.

It has been proposed that complex morphology help to protect against a hostile environment, and the observation that some strains switch to simple morphology after a small number of passages on rich media (i.e. favorable conditions) may support this hypothesis. It has been observed that starvation results in reorganization of yeast colonies at the cellular level, and there is evidence that budding patterns and distributions of cell shape are different in complex colonies than simple colonies (Voordeckers et al., 2012).

The key cellular factors that contribute to the morphogenesis of complex colonies are still largely undefined. Factors such as strength of adhesion, bud location, cell shape, spatially and temporally variable rates of cell division and cell death, secretion of extracellular matrix, and other such variables must contribute in some way to establishing and maintaining colony architecture during colony growth.

We investigated colony shapes of *catp* harboring strains in order to verify: i. if and how their morphology changes depending on carbon source and metabolic conditions, and ii. if different *catp* alleles contribute to colony morphology reshaping. Colony morphology was observed and photographed through a binocular microscope both in SD media containing glucose and glycerol alternatively, and in addition to Trypan blue, that selectively stain dead cells, to evaluate cell vability.

Each strain growing on Glucose makes round smooth colonies (Fig.16), as is typical.

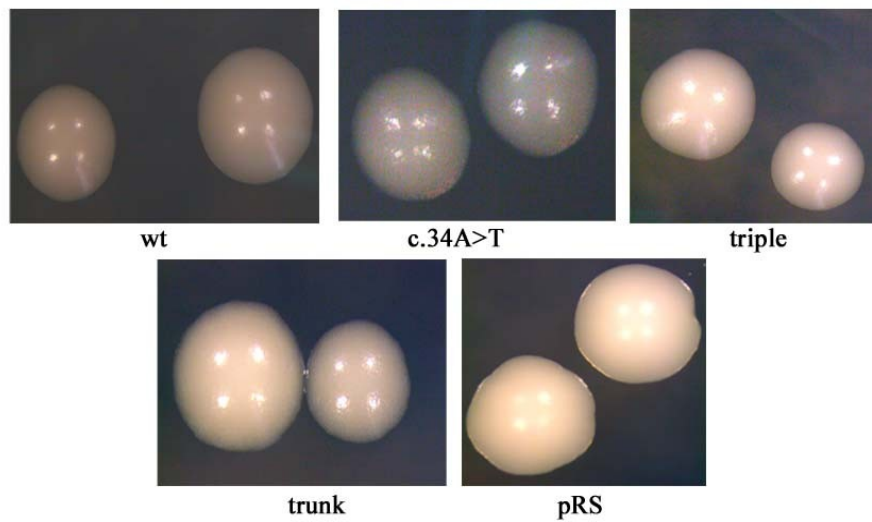


Fig. 16 Colony morphology on Glucose medium: smooth colonies

When grown on non fermentative medium, such as glycerol, negative control forms wrinkly colonies, and the same grown phenotype was observed for strain harboring *catp* c.34A>T mutant. Surprisingly, *wt*-transformed strain and also *triple* and *trunk* mutants did not form the expected wrinkly/fluffy colonies; rather, colony morphology was more similar to the smooth phenotype. It may be seen that the surface of colonies is not perfectly smooth but fail to form wrinkly colonies (Fig.17).

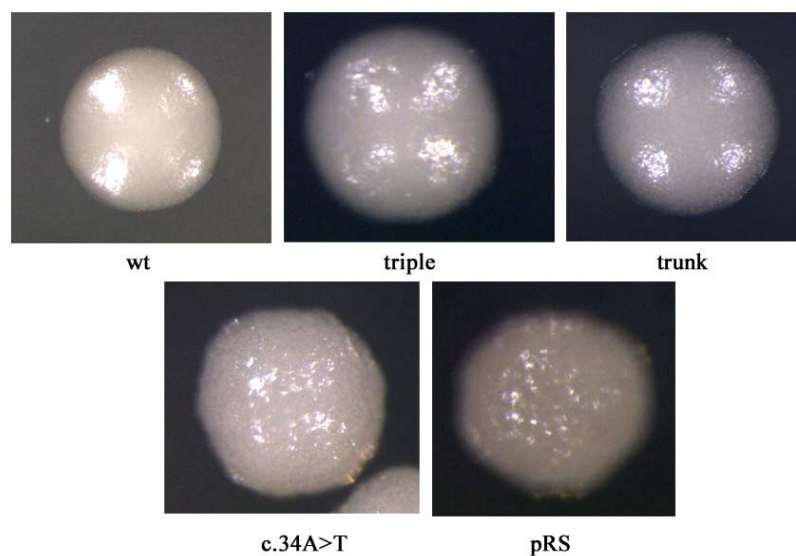


Fig. 17 Colony morphology on Glycerol medium: wrinkly colonies (pRS and c.34A>T mutant).

A similar experiment was done adding Trypan blue as a vital stain to SDGlu agar. Colonies grew smooth and white, except for chimp allele, which appears flat and with irregular edges; stain uptake is strong, especially at the colony center (Fig.18). The uptake of Trypan blue by colonies' core is indicative of massive cellular death where growth conditions are subjected to limitations.

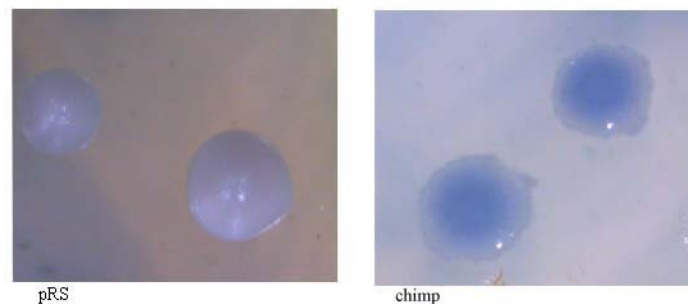


Fig. 18 SDGlu-TB plates details.

When SDGly medium was used, different results arose. Both size and shape of wild type colonies are different from negative control and c.34A>T mutant. Wild type colony surface is smooth, while c.34A>T mutants colonies are bigger and wrinkly, alike negative control (Fig.19). Other mutants share the same colony phenotype with *wt*.

Images were then elaborated by a dedicated software - ImageJ - which was able to measure Trypan blue distribution throughout colonies (Fig.20). Stain distribution appears uniform in wrinkly/fluffy colonies, suggesting that dead cells are homogeneously distributed throughout the whole colony. On the contrary, the edges of smooth colonies are transparent since the blue cells are concentrated in the core region of the colonies, meaning that active cells proliferation predominantly occurs at colony margins where growth is maximal.

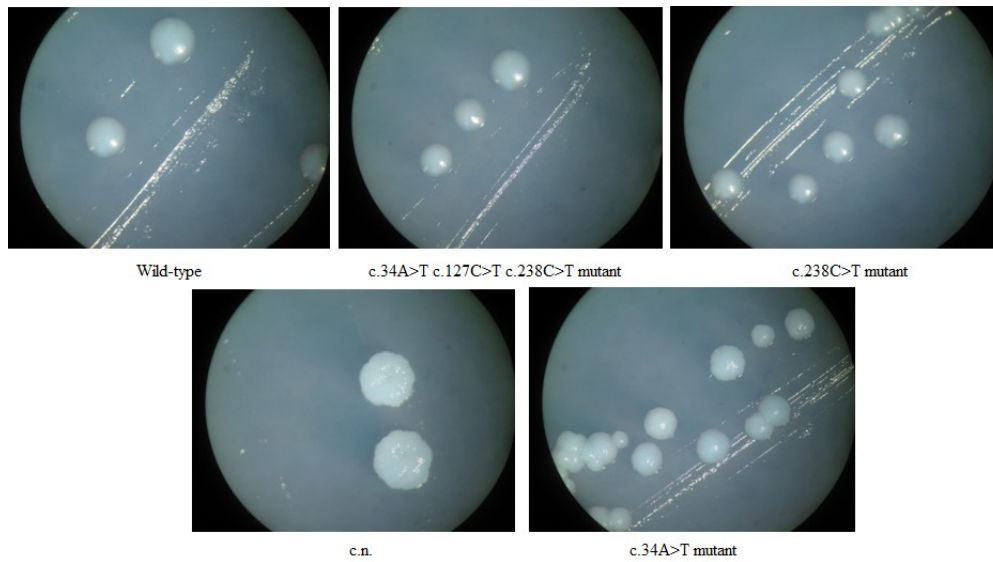


Fig. 19 SDGly-TB medium

These results are compatible with a differential action, or role, of *catp* alleles, and suggested that c.34A>T behaves differently with respect to others alleles. It is of great interest that the phenotype of the *triple* mutant, which also contains the c.34A>T mutation, is reverted to the *wt* one.

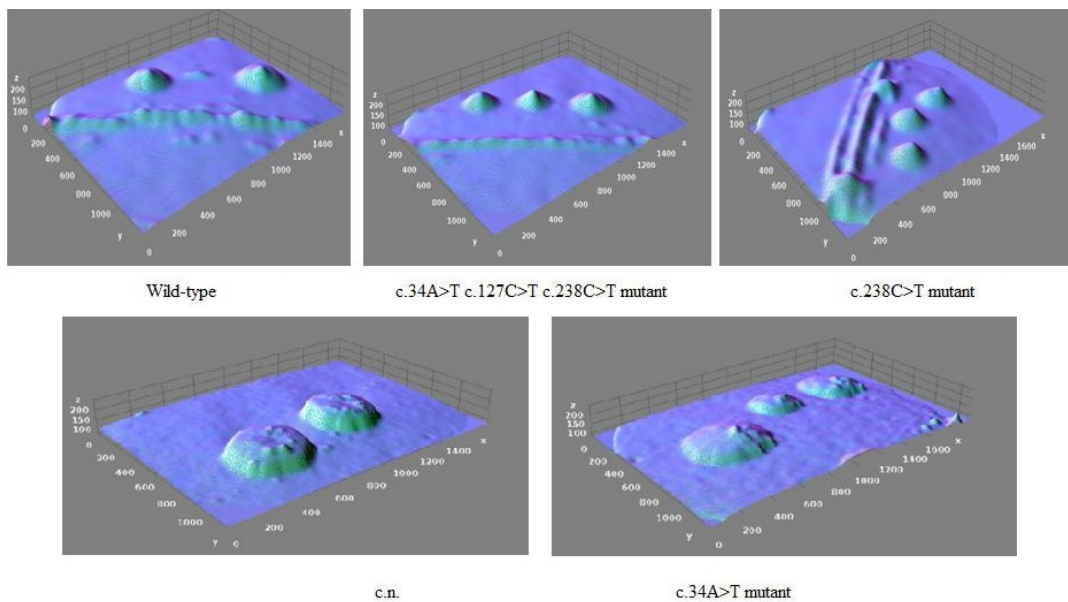


Fig. 20 ImageJ elaborated colonies images.

Once again, the strain harboring the chimp-allele differs from the others when grown on SDGly; I found only colonies of large size, but exhibiting high uptake of TB, suggesting high death rate (Fig.21).

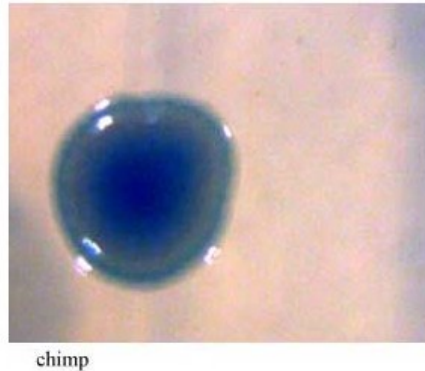


Fig. 21 SDGly-TB plate detail of chimp allele

CATP protein seems able to affect yeast growth properties, both in positive and in negative ways, probably interacting with cell metabolism. Different alleles confer to their host distinguishable growth phenotypes.

Furthermore, colonies morphology of others mutants can suggest that c.127C>T mutation can act as suppressive mutation that counteracts the phenotypic effects of c34A>T mutation. This hypothesis will be addressed when the double mutant will become available.

Investigation upon yeast complex morphologies formation arises a series of unanswered questions around the biological role of colony morphology. It is tempting to speculate that the intricate *hub-and-spokes* patterns of colony surface may help carrying water and nutrients from the substrate through the colony, and that the wrinkly surface of a colony may help to increase the surface area for gas exchange. Changes in the expression of a large number of genes involved in respiration (mitochondria, respiratory chain, ion homeostasis and oxidation/reduction) indicate that the wrinkly colony surface may influence the balance between respiration and fermentation (Váchová and Palková,

2011). It is possible that *catp* expression with its allelic variants interferes with colony shape establishment during its formations.

Effects of Hydrogen peroxide-mediated oxidative stress

The results of growth in glycerol suggested that *catp*-transformed strains were become sensitive to some oxidative stress. I further tested this hypothesis by adding H_2O_2 to yeast cultures for one hour before plating on YPDA-agar. Yeast strains carrying the wt allele, the c.34A>T allele and the vector pRS415 only as negative control were pre-grown in SD+glycerol, splitted into two aliquots and one of them treated with 0.25mM H_2O_2 . After one hour, six serial dilutions were dropped into agar plates (Fig.22).

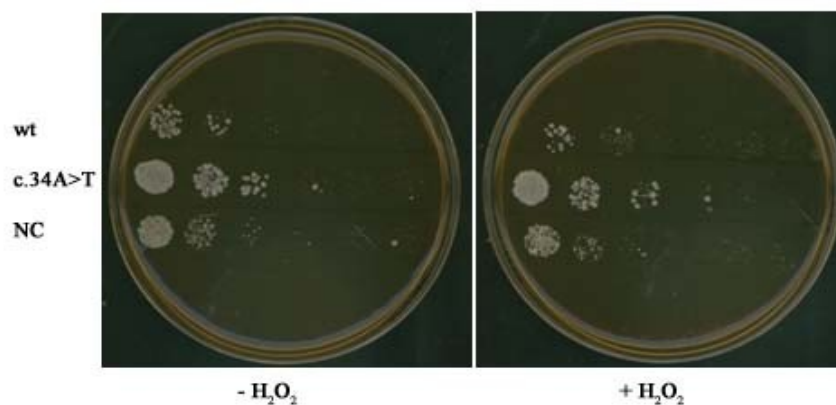


Fig. 22 Hydrogen peroxide-mediated inhibition

It could be observed that *wt* harbouring strain grew poorly and was more sensitive to H_2O_2 than others strains. The c.34A>T-transformed strain showed best growth rate and outperformed even the negative control. It is only slightly inhibited by H_2O_2 .

These results agreed with preliminary experiments done on *E.coli* (not shown), and, together with former results on growth properties, suggested that the biological role of *catp* is concerned with oxidative stress.

The Warburg effect in yeast strains harboring *catp* alleles

In the 1920's Otto Warburg described the most common biochemical phenotype of tumor cell: even in presence of a normal oxygen level, glycolysis is highly elevated and accompanied by high lactate production as well as drastically reduced mitochondrial respiration (Warburg, 1956).

Fermentation, and a concomitant decrease in mitochondrial respiration, occur in rapidly proliferating yeasts in a manner similar to tumor cells. The Crabtree positive yeasts, like *S. cerevisiae*, can switch on and off respiration depending on changes in carbon source (Ruckenstuhl *et al.*, 2009). This ability allows to perform media shift experiment to mime cancers cell metabolism and to evaluate *catp* alleles effect on yeast growth property.

We know that programmed cell death, which protects against cell transformation and tumorigenesis, is associated to a number of mitochondrial processes in mammalian cells. Equally, yeast cells undergo programmed cell death in a mitochondria-depending manner. Therefore cell death, oxidative phosphorylation, yeast colonies growth and tumor growth can be correlated. *S.cerevisiae* possesses a unique glucose repression system that upon growth on glucose drastically suppresses respiration independently of oxygen availability (Hausmann *et al.*, 1976).

I tested yeast strains carrying different *catp* alleles in modifying the growth of yeasts in SD containing 2% glucose. After 1 day of incubation at 30°C, cultures were diluted to 10^4 /ml and plated on SD containing, alternatively, 2% glucose, 2% galactose or 3% glycerol as carbon sources. Growth properties and size of colonies were then examined. Colonies plated on SDGly showed a delay in growth compared with colonies on SDGlu and SDGal medium. After 4 days, CFU count was performed and results are summarized in the following graphic, normalized to glucose's values (Fig.26). Since respiration is either suppressed (SDGlu), cooperatively active with fermentation (SDGal), or it represents the exclusive energy source (SDGly), data can be explained taking into account that suppression of colonies growth can be ascribed to an immediate ROS burst (Ruckenstuhl *et al.*, 2009).

The negative control, i.e. yeast transformed with empty pRS415 vector, showed a decrease in colony number when grown on plates with different carbon source. A decrease of 40% and 56% was obtained in Galactose and Glycerol, respectively, in comparison to standard Glucose plates. This reductions are in close agreement with results of Ruckensthul et al. (2009).

On the contrary, the yeast strain carrying the *wt* construct, suffers some stress. Its growth seems deeply impaired even on Galactose or Glycerol, since up to 80% and 90% of cells, respectively, are lost. The c.34C>T mutant exhibits a certain tolerance to stress triggered both by galactose and glycerol. *Triple* mutant is very tolerant to stress, while the *Trunk* allele shows a different, peculiar behavior (Fig.23).

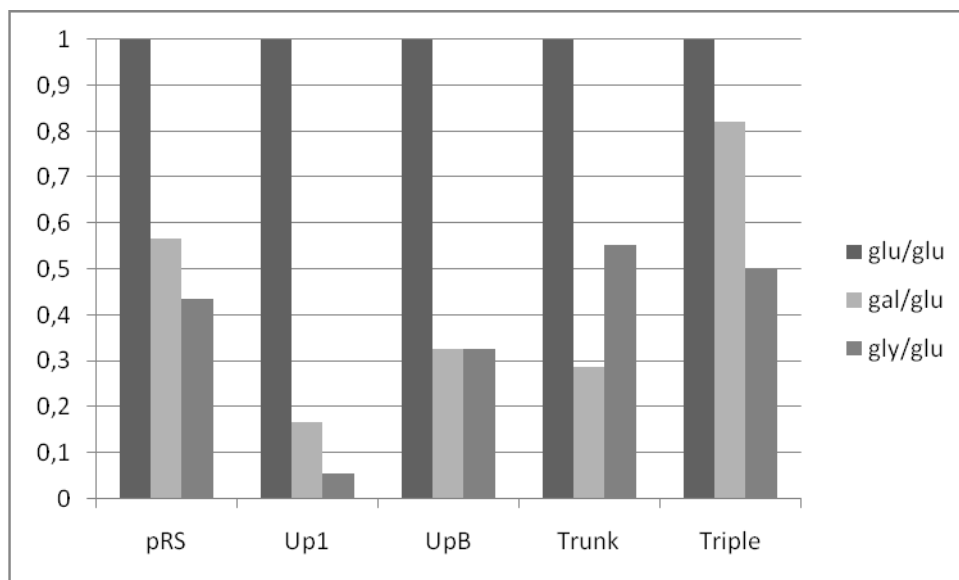


Fig. 23 CFU counts after media shift

As a further analysis, the size of colonies grown on SDGlu media was measured (Fig.24). The wild-type construct produces colonies significantly larger than others, which share a similar colony size among them (t-test: 11,3; 18 degrees of freedom; p=0).

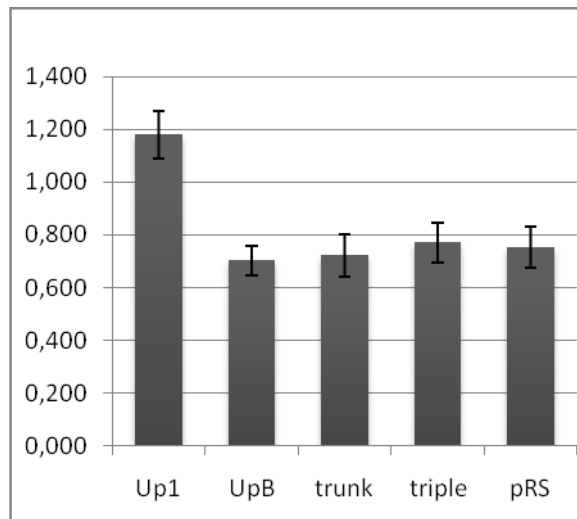


Fig. 24 Colonies size on SDGlu.

I conclude that *wt* allele outperforms other alleles on high glucose, but suffers very much on respiration-triggering media, such as Galactose and Glycerol, perhaps because it is not able to cope with the stress. Thus, it seems that the *wt* allele is better fitted for tumour growth, as long as the Warburg effect is established.

Effects of CATP on yeast growth properties under oxidative stress

In order to verify if oxidative stress is at the base of the growth behavior of *catp* alleles, I verified ROS production in different growth conditions.

Alternative carbon sources determined meaningful differences in growth. Significant data emerged from ROS production analysis obtained upon growth in liquid medium containing glycerol or glucose. ROS production was measured both in absence and after treatment with 0,25mM H₂O₂. ROS levels were assessed by fluorescence measurement; since H₂O₂ treatment was toxic for yeast cells, fluorescence values were normalized to DNA content (Fig.25). For this reason, only fluorescence/DNA ratios are considered.

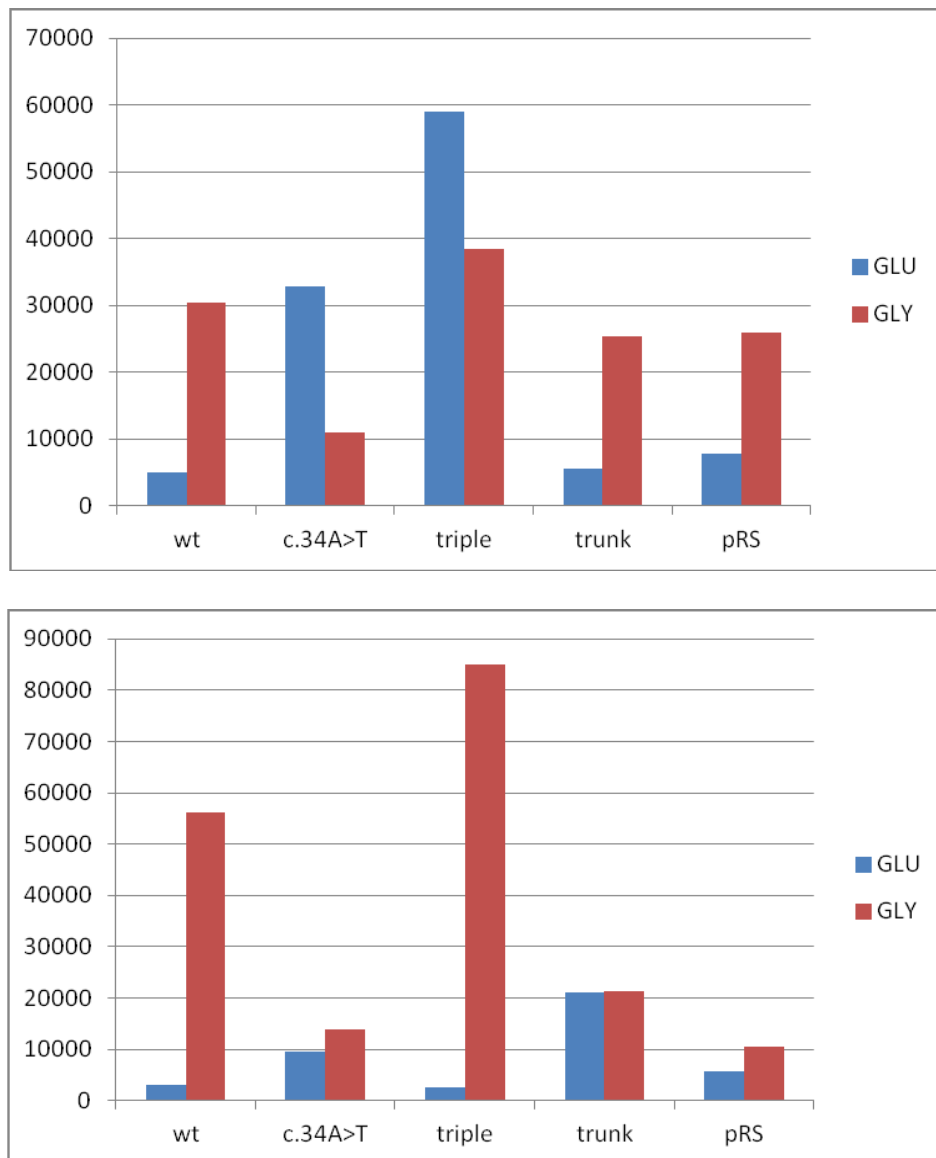


Fig. 25 ROS production without (up) and after (down) H₂O₂ treatment

An obvious difference in ROS production can be seen in H₂O₂ treated vs. untreated cultures, even if the most interesting observations emerge from the comparison of ROS level produced by clones after H₂O₂ treatment. Each allele showed an increase in ROS production in Glycerol whose magnitude is, however, allele depending. In such conditions, *wt*-transformed strain exhibits a very marked enhancement compared to negative control (pRS). Again, c.34A>T is more stress-tolerant in absence of H₂O₂, but this behavior is reversed following H₂O₂ treatment. *triple*-transformed strain behaves in a superimposable, but even enhanced, way with respect to c.34A>T. *trunk* allele did not differ in glucose or glycerol when treated, but otherwise it shows an inverse pattern of ROS production.

From these results, I could confirm that differential ROS production is at the base of oxidative stress sensitivity of *catp* alleles. From a genetic point of view, it is to be noted that same mutations influenced growth phenotypes and ROS production in different ways if alone or in associated with each other. For example, the *trunk* mutation c.238C>T alone confirmed a characteristic 'inverse' pattern already observed in the context of the Warburg effect, but contributed to reverse the phenotype in the *triple* mutant. Ongoing experiments in our laboratory seem to confirm that this mutation greatly affects host chronological lifespan.

DISCUSSION

The results so far available suggest that the use of a yeast model is a promising approach for the study of *CATP* functions.

Colony morphology confirms that the 79C>T mutation, giving rise to a very rare Cys triplet in human, is indeed selectable, since a negative influence of chimp allele on yeast growth has been found. Colony growth is severely impaired and shown a dissimilar phenotype compared to human alleles. More phenotypic assays are required to define chimp allele activity.

Yeast colony morphology are deeply influenced by transformation with *catp* human alleles. c.34A>T mutant gives the most divergent phenotype compared to other alleles in respiratory environment, where its expression is clearly crucial for the organization of cells into colonies, reflecting metabolic, ion homeostasis and oxidative conditions of the growing-forming colony yeast.

In particular, ROS assay resulted very promising, since shows how yeast strains produce/regulate ROS level in a way that is strictly alleles depending. *wt* allele bestows on yeast a major sensitivity to respiratory metabolism which is expressed by a burst of intracellular ROS.

The Warburg effect-like condition of growth, i.e. yeast grown on glucose 2% where fermentation takes exclusive place, suggest a synergic activity of *wt* protein with Warburg effect, while shifting to respiratory medium suggests an opposite behavior highlighting a stress due to ROS production.

My results on yeast model suggest that the c.34A>T mutant would modify the fitness of the yeast strain, and that the triple and, presumably, the double mutant allowed to override this effect and restore growth properties similar to the wild type. In absence of further functional data, these data indeed suggest an important role for *CATP* even in human cells and tissues.

Chapter 5

CONCLUSIVE REMARKS

The study of *catp* has to face three main clues. First, the gene maps within the RMD at 6q27, which is thought to contain either a tumor suppressor gene, or a senescence gene, or a gene with both properties. Second, the cDNA was isolated from fetal brain, a tissue not closely related, from a developmental point of view, to those where tumors developed. Third, it lacks any homology with known genes/proteins, and evolutionary evidences show that it is a *novel gene*.

I have to mention here that a possible role of *CATP* in ROS production may be of biological relevance both in cancer and in neurodegenerative disorders. A functional analysis of the role of each allele was undertaken and led to some surprising results. For example, *S.cerevisiae* grown in 2% glucose mimics the well known Warburg effect in cancer (Ruchenstul, 2009; Warburg, 1956). The high glucose medium allowed yeast to grow using exclusively glucose fermentation with suppression of mitochondrial respiration, so that less ROS are produced. Growth of wild type allele in 2% glucose is very enhanced compared to both control and other alleles, suggesting that wild type allele contributes to yeast growth in fermentative-only conditions; however, it also lead to impaired growth in the presence of ROS, which occurs in mixed fermentative-respiratory conditions (in galactose plates) or true respiratory conditions (in glycerol plates) (see Ruckenstul, 2010).

CATP proteins, either wt or mutant, are directly involved in growth and ROS production. The presence of different alleles may influence, in a manner not fully clear, the behavior of cells subjected to oxidative stress. In this way, the biological role of wt allele would be compatible with enhanced sensitivity of cells to ROS production which has been shown to occur in neurodegenerative disorders, cancer and aging.

c.34A>T mutant may contribute to the growth in presence of stress, in conditions where wt allele would eventually led to cell death or cellular aging. Further SNPs accumulated in c.34A>T mutant led to proteins more compatible with *wt* functions. An obvious conclusion is that c.34A>T was subjected to selection since it would led to unfavorable phenotype. It is to be mentioned that I never found any

occurrence of c.34A>T homozygotes, estimated to be about 0,36% by Hardy-Weinberg law, even if about 1000 alleles, including normal and affected individuals, were scored. It is possible that those homozygotes are underrepresented in normal population or restricted to some disease, so far not included in our search.

Since both cancer and neurodegenerative disease are multi-factorial condition which involve gene networks, the *in vivo* effect of *catp* could be influenced by further interactions. Taking into account this consideration, it is possible that CATP variants effects *in vivo* could be related to ROS scavenging, a role they possibly share with cellular metallothioneins.

Chapter 6

MATERIALS AND METHODS

DNA samples.

Genomic DNA samples from 90 Burkina Faso women, described in a paper of Musumeci *et al.* (2009) were kindly provided by Dr. Musumeci through I.R.M.A (Acireale, Italy).

Genomic DNA from Alzheimer patients and from Epilepsy with earlier onset patients were kindly provided by I.R.C.S.S. Oasi Maria SS of Troina (Italy).

Genomic DNA from 12 Autism Spectrum Disorder were kindly provided by Dr. G. Zaccarello, Department of Medical Sciences; University of Torino, Italy

Genomic DNA samples from Acute Myeloid Leukemia patients were kindly provided by Prof. D. Condorelli and by Lab. Biologia Molecolare U.O. Ematologia Presidio Ospedaliero Ferrarotto Alessi - Azienda Ospedaliero-Universitaria "Policlinico - Vittorio Emanuele", Catania, Italy.

Direct cDNA selection

Direct cDNA selection is realized by hybridization of fetal brain cDNAs library constructed in λ gt10 with YAC911C10 (Lovett, 1991).

Denaturing High-Performance Liquid Chromatography (DHPLC)

Denaturing High-Performance Liquid Chromatography (DHPLC) analysis was performed with Wave 3500HT DNA-fragment analysis system (Transgenomic). PCR products were eluted in 5% acetonitrile gradient with a flow of 1.5 ml/min. Buffer gradient values (buffer A, 0.1 M TEAA; buffer B, 0.1 M TEAA/ 25% acetonitrile), starting and ending point for the gradient, melting temperature were predicted by Navigator software (Transgenomic). Heterozygous and homozygous profiles were identified as different elution peaks.

Phasing

To establish the phase of SNPs identified, PCR products of interest (cap_13fw CACACGCTGAGTTTTCTGTGT, cap_13rev GAAAAGAGCTGTCAGGCCCA) are cloned using PCR kit TOPO TA cloning: pCR 2.1-TOPO vector and *E. coli* TOP-10 genotype F- mcrA Δ (mrr-hsdRMS-mcrBC) ϕ 80lacZ.M15 .lacX74 recA1 araD139 galU galK (ara-leu)7697 rpsL (StrR) endA1 nupG (Invitrogen).

Sequencing

For sequencing Big Dye Terminator chemistry (Applied Biosystems) and automated sequencer ABI3130 (Applied Biosystems) are used.

SNP Genotyping Assay.

Custom SNP Genotyping Assay was designed, by submitting target sequences of interest (Applied Biosystems®, Assays-by-DesignSM Service for SNP Genotyping Assays - TaqMan® MGB probes, FAM[™] and VIC® dye-labeled). End point read RealTime PCR (StepOne[™] Real-Time PCR Systems), was performed with TaqMan Chemistry (Applied Biosystems®, TaqMan® Fast Universal PCR Master Mix, No AmpErase® UNG) in high purified genomic DNA (10-20ng/ μ l). Data were analyzed with dedicated software for allele calls and conversion to genotype (TaqMan® Genotyper Software).

Bioinformatic tools

dbSNP short genetic variations database (<http://www.ncbi.nlm.nih.gov/snp/>).

Comparison between human, chimpanzee and orangutan is realized using the genome browser (<http://genome.ucsc.edu/index.html>), comparison between human, chimpanzee and gorilla is achieved through ensemble genome browser (<http://www.ensembl.org/index.html>).

Region of interest are aligned by Clustal omega - Multiple sequence alignment (<http://www.ebi.ac.uk/Tools/msa/clustalo/>).

For bioinformatic analysis of *CATP* protein sequence, Expasy (**SIB Bioinformatics Resource Portal**) software tools are used (<http://www.expasy.org/>).

Designing a synthetic peptide for *CATP*.

The 17-mer synthetic peptide MRNETQNITRSHLSQRC was designed on the alpha-helical domain present in the N-terminal moiety of *CATP*. Peptide conjugation to ovalbumin was carried out through the peptide amino terminal using glutaraldehyde, as previously described (Reichlin, 1980).

Polyclonal and monoclonal antibodies.

For polyclonal antibody production, two mice were inoculated intraperitoneally using alumina powder as adjuvant (Chase, 1967). After 3 weeks, mice were boosted with the same antigen and killed after one more week by intracardiac perfusion, in agreement with national and local legislations regulating animal health care. Sera were checked by dot blot analysis for affinity towards the peptide before use in immunoassay.

For monoclonal antibody production, the same peptide was sent to Inbiolabs (Tallinn, Estonia), a biotec company specialized in immune research, in order to make hybridomas. Five of them (4A7, 2G1, 5C6, 8A2, G1) which gave positive results were inoculated in mice in order to produce ascites. 6 to 14 mg crude IgG (subtype G1) were obtained for each hybridoma.

Cell culture.

Human SH-SY5Y neuroblastoma cells were grown in RPMI 1640 media (Cellgro) containing 10% heat-inactivated horse serum (Gibco BRL), 5% heat-inactivated Fetal Clone II (Hyclone, Logan, UT), 2 mM L-glutamine, and 100 U/ml penicillinG-streptomycin.

Immunocytochemistry.

Slides with normal and pathological human tissues were obtained from Anatomic-Pathology unit of Cannizzaro Hospital (Catania) as paraffin-embedded 5 μ m slices. For immunohistochemical analysis, slides were deparaffinized, rehydrated, subjected to three 5 min cycles in a microwave at 360 W in citrate buffer, pre-incubated in 3% H₂O₂ in citrate buffer pH 6, and thoroughly washed in 50 mM Tris-Cl (pH 7.4), 150 mM NaCl (TBS) containing 0.05% Tween 20. (washing buffer). Slides were then pre-incubated with 3% bovine serum albumin (BSA) in TBS for 30 min, incubated with 1 : 200 dilution of the antibody in TBS containing 1% BSA, thoroughly washed in washing buffer before revelation with the LSAB 2 kit (anti-mouse, biotinylated and peroxidase-labelled streptavidin) and 3,3'-diaminobenzidine-4HCl (DAB; Dako, Carpinteria CA, USA) from Dako, following the instructions contained in the kit. When necessary, sections were counterstained with haematoxylin after revelation, dehydrated and mounted in xylene-based DPX mountant (BDH, Pool, UK). For negative control, antibody dilutions were incubated with the immunizing peptide (100 ng) for 1 h before applying to the slides.

Immunofluorescence.

SH-SY5Y cells seeded on 4-well Lab-Tek™ II Chamber Slide™ System (Nunc International Corporation, Naperville, IL). The following steps were conducted at room temperature (~25°C) in the dark unless otherwise indicated and all of the solutions were made in PBS. Cells were fixed using 4% paraformaldehyde for 10 min, washed with PBS, treated with 100 mM glycine for 15 min, permeabilized with 1% Triton X-100 for 1 min, and rinsed three times with PBS prior to incubation with 5% FBS for 1 h at 37°C to reduce the background. Cells were incubated overnight with a cocktail of 5 monoclonal antibodies (1:200) in 10% FBS. Cells were rinsed three times with PBS and incubated for 3 h with 488 Alexa anti-mouse IgG secondary antibody (1:5,000; Molecular Probes) in 5% FBS. Cells were rinsed three times with PBS and incubated for 30 min with 4',6-diamidino-2-phenylindole (DAPI, 1:10,000; Sigma) in 5% FBS. Slides were washed extensively in PBS prior to coverslip mounting with Immun-mount (Shandon). Cells were visualized using a Nikon Diaphot 200 epifluorescence microscope and a Digital Spot CCD camera (Diagnostic Instruments) was used to capture images.

Yeast host

Yeast strain used is wtFF18733 (Mat **a**, *leu2-3-112*, *trp1-289*, *his7-2*, *ura3-52*, *lys1-1*).

Cloning

Cloning vector used is shuttle plasmid pRS415 (Fig.26 - Tab.4).

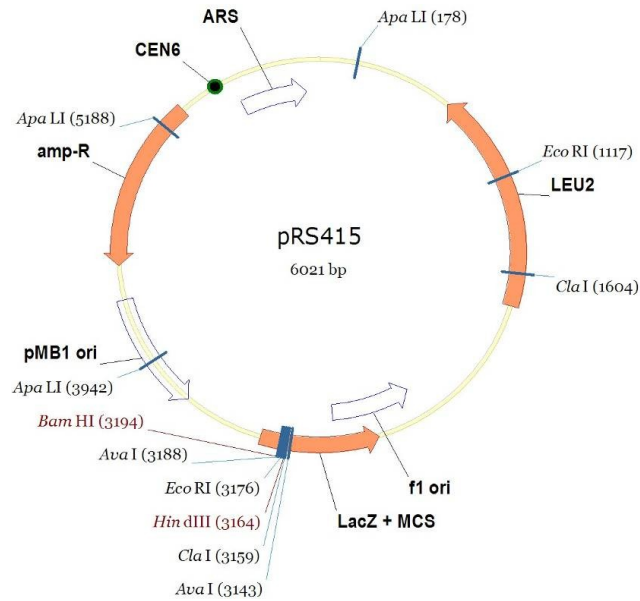


Fig. 26 pRS415 map

LEU2 CDS
f1 origin of replication (+ -)
lacZ alpha CDS/multiple cloning site
pMB1 origin of replication (counterclockwise)
beta-lactamase (bla; amp-r) CDS
beta-lactamase signal peptide CDS
CEN6 (yeast centromere sequence)
Histone H4 ARS (autonomously replicating sequence)

Tab IV pRS415 main features

A pool of yeast transformed strain with each of *catp* alleles was accomplished by directional cloning (BamHI-HindIII) in order to assure the correct frame. PCR product purified was cloned, thanks to restriction site added with the primers, into pRS415 plasmid: *_bam* (CTTGGATCCCATGTTGCTGCTCTGGTTG) and *_hind* (GTTAAGCTTGGTGTGTTCTTATCACAT). Site-specific mutagenesis Site-specific mutagenesis was performed through bridged-PCR. Inner primers used are

chimp_fw (AGCCAGCGGcGCTGC) and chimp_rev (TCGCCgCGACGACACT), outer primers are them mentioned above. PCR is performed with inner primer at lower concentration, after some cycles reaction is forced to continue with the outer primers. PCR product was also cloned into pRS415 plasmid.

Transformation

S.cerevisiae FF18733 wild type stain was transformed by LiAc Mediated method using 100mM LiAc in TE and PEG/LiAc (40% PEG 3350 + 100mM LiAc in 1x TE) solutions.

Yeast culture

Yeast were grown in YPDA medium (Bacto yeast extract 20g/L - Bacto peptone 40g/L - Glucose monohydrate 40g/L - Adenine hemisulfate 80mg/L - Bacto Agar (for making YPDA/agar plates) 20g/L) and in SD minimal medium (Yeast Nitrogen base Difco - aminoacids free - 6,7 mg/ml; Drop-out solution Leu⁻ 1X; glucose 2% /galactose 2% /glycerol 2-3%; agar 20mg/ml).

To vital staining assay, Trypan Blue was added to a final concentration 10 μ mol/L. (Kucseraa, 2000). To Warburg effect assay, carbon source used were glucose 2%, galactose 2% and glycerol 3%.

For ROS dosage H₂O₂ (final concentration 0,25mM), Dichlorodihydrofluorescein diacetate (H₂DCF-DA) and digitonin are used. Emission spectrum were achieved by excitation wavelength 488nm and emission wavelength 520nm (Jakubowski and Bartosz, 2000).

ACKNOWLEDGEMENTS

Prof. Marco Fichera, Drs. Michele Falco, Michele Salemi and Lucia Grillo, Lab. Diagnosi Genetica I.R.C.C.S. Oasi Maria SS. Troina, Italy.

Dr. Zaccarello G., Department of Medical Sciences; University of Torino, Italy.

Dr. Insirello E. for Burkina Faso DNA samples, I.R.M.A. of Acireale, Catania, Italy.

Dr. Tibullo D. Lab. Molecular Biology U.O. Ematologia Presidio Ospedaliero Ferrarotto Alessi - Azienda Ospedaliero-Universitaria "Policlinico - Vittorio Emanuele", Catania, Italy.

Prof. Condorelli D., Drs. Baresi V., Musso N., for AML DNA samples, Department of Chemical Sciences. University of Catania, Italy.

Prof. Guido De Guidi, Department of Chemical Sciences., University of Catania, Italy.

Dr Maria Antonietta Buccheri, National Research Council. Institute for Microelectronics and Microsystems IMM, University of Catania, Italy.

REFERENCES

Amiel, A., Mulchanov, I., Elis, A., Gaber, E., Manor, Y., Fegin, M., et al. (1999). Deletion of 6q27 in chronic lymphocytic leucemia and multiple myeloma detected by fluorescent in situ hybridization. *Cancer Genetic and Cytogenetic*, 112(1):53-6.

Arnold K., Bordoli L., Kopp J., and Schwede T. (2006). The SWISS-MODEL Workspace: A web-based environment for protein structure homology modelling. *Bioinformatics*, 22,195-201.

Aylwyn Scally, Julien Y. Duthiel, LaDeana W. Hillier, Gregory E. Jordan, Ian Goodhead, Javier Herrero, Asger Hobolth, Tuuli Lappalainen, Thomas Mailund, Tomas Marques-Bonet, Shane McCarthy, Stephen H. Montgomery, Petra C. Schwalie, Y. Amy Tang, Michelle C. Ward, Yali Xue, Bryndis Yngvadottir, Can Alkan, Lars N. Andersen, Qasim Ayub, Edward V. Ball, Kathryn Beal, Brenda J. Bradley, Yuan Chen, Chris M. Clee, et al. Insights into hominid evolution from the gorilla genome sequence *Nature*. ; 483(7388): 169–175.

Banga, S. S. (1997). SEN6, a locus for SV40-mediated immortalization of human cells, maps to 6q26-27. *Oncogene*, 14(3): 313-21.

Behrens María I., Roe Catherine M. and Morris John C.. Inverse Association between Cancer and Dementia of the Alzheimer's Type Neurodegenerative Diseases: From Molecular Concepts to Therapeutic Targets. Nova Science Publishers, Inc Ch IX, pp. 111-120

Bennett DA, Leurgans S (2010) Is there a link between cancer and Alzheimer disease? *Neurology* 74: 100–101.

Benz Christopher C. and Yau Christina. Ageing, oxidative stress and cancer: paradigms in parallax *Nat Rev Cancer*. 2008 November; 8(11): 875–879.

Bodnar AG, Ouellette M, Frolkis M, Holt SE, Chiu CP, Morin GB, Harley CB, Shay JW, Lichtsteiner S, Wright WE. 1998. Extension of life-span by introduction of telomerase into normal human cells. *Science* 279: 349–352.

Botstein D, Steven A. Chervitz, Michael Cherry. Yeast as a Model Organism. *Science* 1997: Vol. 277 no. 5330 pp. 1259-1260.

Calabrese V, Mallette FA, Desche[^]nes-Simard X, Ramanathan S, Gagnon J, Moores A, Ilangumaran S, Ferbeyre G. 2009. SOCS1 links cytokine signaling to p53 and senescence. *Mol Cell* 36: 754–767.

Campisi J. 2005. Senescent cells, tumor suppression, and organismal aging: Good citizens, bad neighbors. *Cell* 120: 513– 522.

Carvalho, B., van der Veen, A., Gartner, F., Carneiro, F., Seruca, R., Buys, C., et al. (2001). Allelic gains and losses in distinct regions of chromosome 6 in gastric carcinoma. *Cancer Genetic and Cytogenetic* , 131(1):54-9.

Coppe' J-P, Patil CK, Rodier F, Sun Y, Mun[~]oz DP, Goldstein J, Nelson PS, Desprez P-Y, Campisi J. 2008. Senescence-associated secretory phenotypes reveal cell-nonautonomous functions of oncogenic RAS and the p53 tumor suppressor. *PLoS Biol* 6: 2853–2868.

D'Adda di Fagagna F. 2008. Living on a break: Cellular senescence as a DNA-damage response. *Nat Rev Cancer* 8: 512– 522.

Davies H, Bignell GR, Cox C, Stephens P, Edkins S, Clegg S, Teague J, Woffendin H, Garnett MJ, Bottomley W, et al. 2002. Mutations of the BRAF gene in human cancer. *Nature* 417: 949–954.

Demetrius LA, Simon DK. 2013 The inverse association of cancer and Alzheimer's: a bioenergetic mechanism. *J R Soc Interface* 10: 20130006.

Dimri GP, Lee X, Basile G, Acosta M, Scott G, Roskelley C, Medrano EE, Linskens M, Rubelj I, Pereira-Smith OM. 1995. A biomarker that identifies senescent human cells in culture and in aging skin in vivo. *Proc Natl Acad Sci* 92:9363–9367.

Franza BR, Maruyama K, Garrels JI, Ruley HE. 1986. In vitro establishment is not a sufficient prerequisite for transformation by activated ras oncogenes. *Cell* 44: 409–418.

Gaidano, G. R. (1992). Deletions involving two distinct regions of 6q in Bcell non-Hodgkin lymphoma. 80(7): 1781-7, Blood.

Giglia-Mari Giuseppina, Zotter Angelika, and Vermeulen Wim. DNA Damage Response. Cold Spring Harb Perspect Biol 2011;3:a000745.

Goffeau A, Barrell BG, Bussey H, Davis RW, Dujon B, Feldmann H, Galibert F, Hoheisel JD, Jacq C, Johnston M, Louis EJ, Mewes HW, Murakami Y, Philippsen P, Tettelin H, Oliver SG. Life with 6000 genes Science. 1996 Oct 25;274(5287):546, 563-7.

Gray-Schopfer VC, Cheong SC, Chong H, Chow J, Moss T, Abdel-Malek ZA, Marais R, Wynford-Thomas D, Bennett DC. 2006. Cellular senescence in naevi and immortalisation in melanoma: A role for p16? Br J Cancer 95: 496–505.

Harley CB, Futcher AB, Greider CW. 1990. Telomeres shorten during ageing of human fibroblasts. Nature 345: 458–460.

Harman D. Aging: a theory based on free radical and radiation chemistry. J. Gerontol. 1956;11:298–300.

Hausmann P, Zimmermann FK (1976) The role of mitochondria in carbon catabolite repression in yeast. Mol Gen Genet 148: 205–211.

Hayflick, L., and Moorhead, P. S. (1961). "The serial cultivation of human diploid cell strains." Exp Cell Res 25:585-621.

Hoeijmakers JH. 2009. DNA damage, aging, and cancer. N Engl J Med 361: 1475–1485.

Itahana Koji, Campisi Judith, Dimri Goberdhan P.. Mechanisms of cellular senescence in human and mouse cells. Biogerontology. 2004;5(1):1-10

Jakubowski W and Bartosz G . 2,7-dichlorofluorescein oxidation and reactive oxygen species: What does it measure? *Cell Biology International* 2000, Vol. 24, No. 10, 757–760.

Kucseraa Judit, K. Y. (2000). Simple detection method for distinguishing dead and living yeast. *Journal of Microbiological Methods* 41 , 19–21.

Kuilman, Thomas ; Michaloglou, Chrysiis ; Mooi, Wolter J. ; et al (2010) The essence of senescence *GENES & DEVELOPMENT* Volume: 24 Issue: 22 Pages: 2463-2479.

L. Lindstrom Derek and Gottschling Daniel E. 2009 The Mother Enrichment Program: A Genetic System for Facile Replicative Life Span Analysis in *Saccharomyces cerevisiae* 10.1534/genetics.109.106229.

Land H, Parada LF, Weinberg RA. 1983. Tumorigenic conversion of primary embryo fibroblasts requires at least two cooperating oncogenes. *Nature* 304: 596–602.

Laschober, G. T., Ruli, D., Hofer, E., Muck, C., Carmona-Gutierrez, D., Ring, J., Hutter, E., Ruckenstein, C., Micutkova, L., Brunauer, R., Jamnig, A., Trimmel, D., Herndler-Brandstetter, D., Brunner, S., Zenzmaier, C., Sampson, N., Breitenbach, M., Fröhlich, K.-U., Grubeck-Loebenstein, B., Berger, P., Wieser, M., Grillari-Voglauer, R., Thallinger, G. G., Grillari, J., Trajanoski, Z., Madeo, F., Lepperdinger, G. and Jansen-Dürr, P. (2010), Identification of evolutionarily conserved genetic regulators of cellular aging. *Aging Cell*, 9: 1084–1097.

Lee AC, Fenster BE, Ito H, Takeda K, Bae NS, Hirai T, Yu ZX, Ferrans VJ, Howard BH, Finkel T. 1999. Ras proteins induce senescence by altering the intracellular levels of reactive oxygen species. *J Biol Chem* 274: 7936–7940.

Levy R. Aging-associated cognitive decline. *Int Psychogeriatr*, 1994;6:63–68.

Libus̃e Va' chova' and Zdena Palkova. Aging and longevity of yeast colony populations: metabolic adaptation and differentiation *Biochem. Soc. Trans.* (2011) 39, 1471–1475.

Lin, H., & Morin, P. (2001). A novel homozygous deletion at chromosomal band 6q27 in an ovarian cancer cell line delineates the position of a putative tumor suppressor gene. *Cancer Lett.* 173: 63–70.

Liu M, Schatz DG. (2009). Balancing AID and DNA repair during somatic hypermutation. *Trends in Imm* 30: 173–181.

Longo, V. D., E. B. Gralla and J. S. Valentine, (1996) Superoxide dismutase activity is essential for stationary phase survival in *Saccharomyces cerevisiae*. Mitochondrial production of toxic oxygen species in vivo. *J. Biol. Chem.* 271: 12275–12280.

Lovett, M. J. (1991). Direct selection: a method for the isolation of cDNAs encoded by large genomic regions. *Proc Natl Acad Sci U S A* , 88(21):9628-32.

Masutomi K, Yu EY, Khurts S, Ben-Porath I, Currier JL, Metz GB, Brooks MW, Kaneko S, Murakami S, DeCaprio JA, et al. (2003). Telomerase maintains telomere structure in normal human cells. *Cell* 114: 241–253.

Miles A. T., Hawksworth G. M., Beattie J. H., and Rodilla V(2000). Induction, Regulation, Degradation, and Biological Significance of Mammalian Metallothioneins. *Critical Reviews in Biochemistry and Molecular Biology*, 35(1):35–70.

Mortimer, R. K., and J. R. Johnston, (1959) Life span of individual yeast cells. *Nature* 183: 1751–1752.

Muntoni, A., Reddel, R.R. (2005). The first molecular details of ALT in human tumor cells. *Hum Mol Genet* 14: R191–R196.

Narita M, Narita M, Krizhanovsky V, Nunˆ ez S, Chicas A, Hearn SA, Myers MP, Lowe SW. (2006) A novel role for high-mobility group a proteins in cellular senescence and heterochromatin formation. *Cell* 126: 503–514.

Negrini M, Sabbioni S, Possati L, Rattan S, Corallini A, Barbanti-Brodano G, Croce CM(1994). Suppression of tumorigenicity of breast cancer cells by microcell-mediated chromosome transfer: studies on chromosomes 6 and 11. *Cancer Res.* Mar 1;54(5):1331–1336.

Passos JF, Nelson G, Wang C, Richter T, Simillion C, Proctor CJ, Miwa S, Olijslagers S, Hallinan J, Wipat A, et al. (2010). Feedback between p21 and reactive oxygen production is necessary for cell senescence. *Mol Syst Biol* 6: 347.

Plun-Favreau H, Lewis PA, Hardy J, Martins LM, Wood NW (2010) Cancer and Neurodegeneration: Between the Devil and the Deep Blue Sea. *PLoS Genet* 6(12): e1001257.

Pollock PM, Harper UL, Hansen KS, Yudt LM, Stark M, Robbins CM, Moses TY, Hostetter G, Wagner U, Kakareka J, et al. (2003). High frequency of BRAF mutations in nevi. *Nat Genet* 33: 19–20.

Rodier F, Coppe' J-P, Patil CK, Hoeijmakers WAM, Munoz DP, Raza SR, Freund A, Campeau E, Davalos AR, Campisi J. (2009). Persistent DNA damage signalling triggers senescence-associated inflammatory cytokine secretion. *Nat Cell Biol* 11: 973–979.

Rubin EH, Storandt M, Miller JP, Kinscherf DA, Grant EA, Morris JC, Berg L.. A prospective study of cognitive function and onset of dementia in cognitively healthy elders. *Arch Neurol*, 1998; 55:395–401.

Ruckenstuhl Christoph, Buttner Sabrina, Carmona-Gutierrez Didac, Eisenberg Tobias, Kroemer Guido, Sigrist Stephan J, Frohlich Kai-Uwe, Madeo Frank (2009). The Warburg Effect Suppresses Oxidative Stress Induced Apoptosis in a Yeast Model for Cancer. *PLoS ONE* February Vol 4 (2), e4592.

Saito, S., & Saito, H. e. (1992). Fine-scale deletion mapping of the distal long arm of chromosome 6 in 70 human ovarian cancers. *Cancer Res* , 52(20): 5815-7.

Sandhu AK, H. K. (1994). Senescence of immortal human fibroblasts by the introduction of normal human chromosome 6. *Proc Natl Acad Sci U S A* , 91(12):5498-502.

Serra-Batiste Montserrat Cols, Neus, Alcaraz Luis A., Donaire Antonio, González-Duarte Pilar, Vašák Milan (2010)The metal-binding properties of the blue crab copper specific CuMT-2: a crustacean metallothionein with two cysteine triplets *JBIC Journal of Biological Inorganic Chemistry*, Volume 15, Issue 5, pp 759-776

Serrano M, Lin AW, McCurrach ME, Beach D, Lowe SW. (1997). Oncogenic ras provokes premature cell senescence associated with accumulation of p53 and p16INK4a. *Cell* 88: 593–602.

Shay JW, Bacchetti S. (1997). A survey of telomerase activity in human cancer. *Eur J Cancer* 33: 787–791.

Shay JW, Wright WE. (2006). Telomerase therapeutics for cancer: Challenges and new directions. *Nat Rev Drug Discov* 5: 577– 584.

Shelton DN, Chang E, Whittier PS, Choi D, Funk WD. (1999). Microarray analysis of replicative senescence. *Curr Biol* 9:939–945.

Stein GH, Beeson M, Gordon L. (1990). Failure to phosphorylate the retinoblastoma gene product in senescent human fibroblasts. *Science* 249: 666–669.

The chimpanzee Sequencing and Analysis Consortium. Initial sequence of the chimpanzee genome and comparison with the human genome. *Nature* 437, 69-87.

Tibiletti, M., Trubia, M., Ponti, E., Sessa, L., Acquati, F., Furlan, D., et al. (1998). Physical map of the D6S149-D6S193 region on chromosome 6Q27 and its involvement in benign surface epithelial ovarian tumours. *Oncogene* , 16(12):1639-42.

Trent, J. M. (1980). Human tumour karyology: marked analytic improvement by short-term agar culture. *Br J Cancer* , 41(6): 867-74.

Voordeckers, K., De Maeyer, D., van der Zande, E., Vincens, M. D., Meert, W., Cloots, L., Ryan, O., Marchal, K. and Verstrepen, K. J. (2012), Identification of a complex genetic network underlying *Saccharomyces cerevisiae* colony morphology. *Molecular Microbiology*, 86: 225–239.

Warburg O (1956) On respiratory impairment in cancer cells. *Science* 124:269-270.

Zhang R, Poustovoitov MV, Ye X, Santos HA, Chen W, Daganzo SM, Erzberger JP, Serebriiskii IG, Canutescu AA, Dunbrack RL, et al. (2005). Formation of MacroH2A-containing senescence-associated heterochromatin foci and senescence driven by ASF1a and HIRA. *Dev Cell* 8: 19–30.

Mizushima N. Autophagy: process and function. *Genes Dev.* 2007;21:2861–2873.

Nakatogawa H, Suzuki K, Kamada Y, Ohsumi Y. Dynamics and diversity in autophagy mechanisms: lessons from yeast. *Nat Rev Mol Cell Biol.* 2009;10:458–467.

Deter RL, De Duve C. Influence of glucagon, an inducer of cellular autophagy, on some physical properties of rat liver lysosomes. *J Cell Biol.* 1967;33:437–449

Glick Danielle, Barth Sandra, and Macleod Kay F. (2010) Autophagy: cellular and molecular mechanisms. *J Pathol* 221(1):3-12.